BŞEÜ Fen Bilimleri Dergisi
6. Cilt - Prof. Dr. Fuat SEZGİN Bilim Yılı Özel Sayısı
74-98, 2019

BSEU Journal of Science
DOI: 10.35193/bseufbd. 567808

e-ISSN: 2458-7575 (http://dergipark.gov.tr/bseufbd)

Araştırma Makalesi / Research Article

Investigations of Structural Properties, Spectroscopic Aspects, Electronic and Thermodynamic Properties of 3-Benzyl-4-[3-(3-methoxybenzoxy)-benzylidenamino]-4,5-Dihydro-1*H*-1,2,4-Triazol-5-one with DFT/HF Basis Sets

3-Benzil-4-[3-(3-metoksibenzoksi)-benzilidenamino]-4,5-Dihidro-1*H*-1,2,4-Triazol-5-on'un DFT/HF Temel Setleriyle Yapısal Özelliklerinin, Spektroskopik Yönlerinin, Elektronik ve Termodinamik Özelliklerinin İncelenmesi

Hilal Medetalibeyoğlu[1*], Haydar Yüksek[2]

Geliş / Received: 20/05/2019 ***Revize / Revised: 23/07/2019*** ***Kabul / Accepted: 31/07/2019***

Öz- Bu makalede, öncelikle 3-benzil-4-[3-(3-metoksibenzoksi)-benzilidenamino]-4,5-dihidro-1*H*-1,2,4-triazol-5-on(1)'un sentezi, FT-IR, NMR kimyasal kaymaları, UV-Vis spektral değerleri incelenmiştir. Daha sonra, molekül 6-311G(d)/3-21G temel setleriyle B3LYP ve HF yöntemleri kullanılarak optimize edilmiştir. Molekülün, elektronik ve termodinamik parametreleri, geometrik ve yapısal özellikleri, HOMO-LUMO enerji değerleri, moleküler elektrostatik potansiyeli (MEP) ve Mulliken atomik yükleri oluşturulmuştur. Bu molekülün ^{1}H-NMR ve ^{13}C-NMR kimyasal kayma değerleri (DMSO çözücüsünde ve temel durumda) GIAO yöntemiyle gerçekleştirilmiştir. Molekülün, geometrik ve spektroskopik parametreleri, 6-311G(d) ve 3-21G temel setleriyle yoğunluk fonksiyoneli (DFT/B3LYP) ve Hartree-Fock (HF) yöntemleri kullanılarak oluşturulmuştur. Ayrıca, FT-IR değerlerinin tayin edilmesinde veda4f yazılım programı kullanılmıştır. UV-vis verileri (etanol ortamında) hesaplanmış ve tüm spektral parametreler deneysel verilerle karşılaştırılmıştır.

***Anahtar Kelimeler*- 4-Amino-1*H*-1,2,4-triazol, 6-311G (d), 3-21G, GIAO, B3LYP, HF.**

***A**bstract*- **In this paper, firstly the synthesis, FT-IR, NMR chemical shifts, UV–Vis spectral values of 3-benzyl-4-[3-(3-methoxybenzoxy)-benzylidenamino]-4,5-dihydro-1*H*-1,2,4-triazol-5-one (1) have been investigated. Later, this molecule was optimized by using B3LYP and HF methods with 6-311G(d)/3-21G basis sets. Electronic and thermodynamic parameters, geometric and structural properties, HOMO-LUMO energy values, the molecular electrostatic potential (MEP) and Mulliken atomic charges of titled molecule have been carried out. ^{1}H-NMR and ^{13}C-NMR isotropic shift values of this molecule (in DMSO solvent and in the ground state) were performed by GIAO method. The geometric and spectroscopic parameters of titled molecule were performed by using density functional (DFT/B3LYP) and Hartree–Fock methods (HF) with the 6-311G(d) and 3-21G basis sets. Also, the determination of FT-IR values was used the veda4f software program. The UV-vis data (ethanol) were calculated and all spectral parameters were compared with experimental data.**

***Keywords*- 4-Amino-1*H*-1,2,4-Triazole, 6-311G(D), 3-21G, GIAO, B3LYP, HF.**

[1]*Corresponding author: hilalmedet@gmail.com (https://orcid.org/0000-0002-1310-6811)
**Kafkas University, Department of Chemistry, Kafkas University, 36100, Kars, Turkey*
[2] Second Author: hhigh61@gmail.com (https://orcid.org/0000-0003-1289-1800)
Kafkas University, Department of Chemistry, Kafkas University, 36100, Kars, Turkey

I. INTRODUCTION

4-Amino-1*H*-1,2,4-triazole and its derivatives play an essential function in numerous biological activities such as antitumor, antimicrobial, anticancer, anti-HIV, antifungal, anti-inflammatory, antiviral, antioxidant and analgesic etc. [1-8]. The synthetic chemistry of the 1,2,4-triazole derivatives is experiencing significant development because of the semiconduction properties of certain materials in this family and because the bioactivity and pharmaceutical application are continuously increasing. In addition, Shiff bases involving 1,2,4-triazole derivative are well founded as significant effective substances in coordination and therapeutic chemistry in literature [10, 11]. In recent years, quantum chemical calculations are commonly used for interpretation, understanding and prevision of experimental results such as geometric parameters, vibrational frequency, absorption/emission measurements, ^{1}H and ^{13}C NMR spectra [8-16]. Furthermore, these calculations are used to determine the optic and electronic properties of organic compounds and to elucidate their structure activity relationship (SAR) [12, 13].

The Density Functional Theory (DFT) and Hartree Fock (HF) methods have been significantly used for the calculation of many parameters of some 4,5-dihydro-1*H*-1,2,4-triazol-5-one derivatives such as structural and spectral parameters; ^{1}H- and ^{13}C-NMR, FT-IR, UV-Vis spectra, HOMO-LUMO energies, Mulliken atomic scharge distributions, thermodynamics and electronic properties. In the literature, the appropriate HF and DFT quantum chemical calculations have been carried out and the findings obtained from the experimental techniques were assessed [17-25].

In this study, 3-benzyl-4-[3-(3-methoxybenzoxy)-benzylidenamino]-4,5-dihydro-1*H*-1,2,4-triazol-5-one (1) were synthesized from the reaction of 4-amino-3-benzyl-1*H*-1,2,4-triazol-5(4H)-one with 3-(3-methoxybenzoxy)-benzaldehyde which was obtained by the reaction of 3-methoxybenzoyl chloride with 3-hydroxybenzaldehyde by use of triethylamine (Scheme **1**). The structural characterization of the compound (**1**) was experimentally accomplished by ^{1}H and ^{13}C NMR, FT-IR and UV-Vis spectral methods [22].

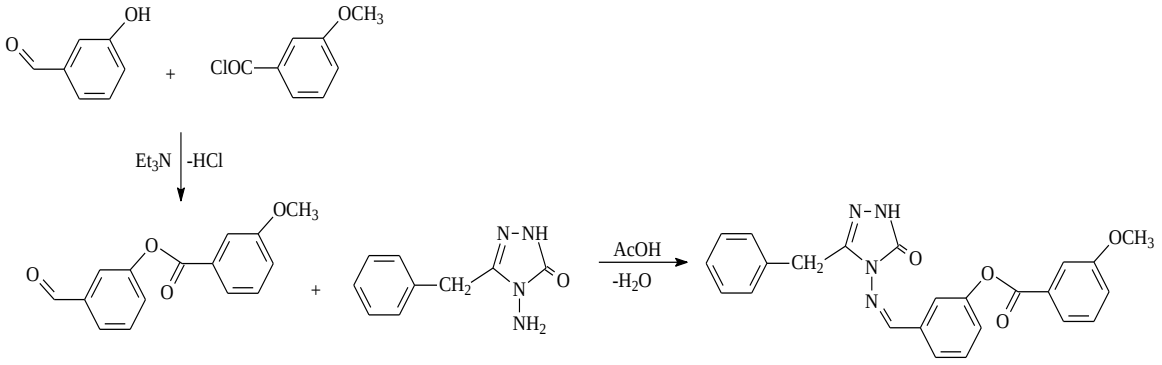

1

Scheme 1. Synthesis route of the compound (**1**)

The compound (**1**) has been optimized through use of B3LYP/HF methods and 6-311G(d) and 3-21G basis sets [22]. This research was carried out to investigate the spectral results, structural framework, between HOMO and LUMO interaction energies and thermodynamic properties. In present study, the geometric parameters, ^{1}H- and ^{13}C-NMR chemical shifts, FT-IR, UV-Vis spectral values, bond angles, total energy, bond lengths, HOMO-LUMO energy values, atomic charges, dipole moment and molecular electrostatic potential (MEP) map of the compound (**1**) were investigated by B3LYP/HF methods and 6-311G(d) and 3-21G basis sets. The experimental findings [22] obtained from UV-Vis, ^{1}H and ^{13}C NMR and FT-IR spectra of the compound (**1**) have been compared with the calculated results by using the same basis sets and methods.

II. MATERIAL AND METHODS

A. Experimental and Spectroscopic values of the compound (1) 3-Benzyl-4-[3-(3-methoxybenzoxy)-benzylidenamino]-4,5-dihydro-1H-1,2,4-triazol-5-one (1)

Yield: 4.23 g (98.72%); mp: 189 ºC; IR (KBr, υ, cm^{-1}): 3167 (NH), 1730, 1698 (C=O), 1578 (C=N), 1273 (COO), 813 and 687 (1,3-disubstituted benzenoid ring), 775 and 687 (monosubstituted benzenoid ring); ^{1}H NMR (400 MHz, DMSO-d6): δ 3.88 (s, 3H, OCH_3), 4.08 (s, 2H, CH_2), 7.21-7.23 (m, 1H, Ar-H), 7.27-7.33 (m, 4H, Ar-H), 7.34-7.38 (m, 1H, Ar-H), 7.46-7.48 (m, 1H, Ar-H), 7.57 (m, 1H, *J*=8.00 Hz), 7.61 (t, 1H, *J*=8.00 Hz), 7.66-7.67 (m, 1H, Ar-H), 7.72-7.76 (m, 2H, Ar-H), 7.77-7.80 (m, 1H, Ar-H), 9.74 (s, 1H, N=CH), 12.02 (s, 1H, NH); ^{13}C NMR (100 MHz, DMSO-d6): δ 31.11 (CH_2Ph), 55.48 (OCH_3), 114.39, 120.23, 120.38, 122.14, 124.86, 125.83, 126.68, 128.38 (2C), 128.83 (2C), 130.10, 130.23, 130.26, 135.23, 135.76, 151.02, 159.46, 146.25 (triazole C3), 151.17 (N=CH), 152.14 (triazole C5), 164.32 (COO); UV λmax (ε): 296 (20.768), 242 (26.677), 220 (26.652) nm.

B. Theoretical Details

In this study, Gaussian09W program were used to calculate the entire structural parameters of the title compound [27]. In the primary, molecular geometry of the title compound was once obtained at the HF and DFT/B3LYP methods and 6-311G(d) and 3-21G basis sets. The received outcomes have been visualized via GaussView 5.0 program [28]. The GIAO (Gauge Including Atomic Orbital) approach is the most extensively used method for calculating NMR shielding values [29]. The determination of FT-IR outcomes were used veda4f software program [30]. The UV-Vis spectra records have been performed by means of time dependent-density functional theory (TD-DFT) and time dependent-hartree fock (TD-HF) methods in ethanol solvent [31]. The optimized molecular parameters (bond angles bond lengths), UV-Vis values, ^{1}H and ^{13}C NMR chemical shifts, FT-IR, total energies, HOMO-LUMO energies, molecular electrostatic potential (MEP) map, mulliken atomic charges and dipole moment of the title compound were investigated. The experimental findings obtained from ^{1}H-/^{13}C-NMR, UV-Vis and FT-IR spectra [26] of the title compound were compared with the calculated results.

III. RESULTS AND DISCUSSION

A. Molecular Geometry

The 3D molecular structure of 3-benzyl-4-[3-(3-methoxybenzoxy)-benzylidenamino]-4,5-dihydro-1*H*-1,2,4-triazol-5-one are shown in (Figure 1). The Mulliken atomic charges, bond lengths, bond angles with the DFT(B3LYP) and Hartree Fock (HF) methods and standard 6-311G(d) and 3-21G basis sets are listed in Table 1-3. The structure optimization and zero point vibrational energy (ZPVE) of the compound are 254.335 (DFT/6-311G(d)), 271.399 (HF/6-311G(d)), 254.484 (DFT/3-21G) and 274.108 (HF/3-21G) kcal/mol. The value calculated for HF is higher than the value of DFT since the ground state energy assumption in HF is more than real energy. The N45-N46, N46=C1, C2=O49 and C2-N47 bond lengths according to HF/DFT methods with 6-311G(d), 3-21G basis sets in the triazole ring are computed as 1.4272/1.3634, 1.3789/1.4387Å, 1.2772/1.2651, 1.2946/1.3110 Å, 1.2187/1.1961, 1.2156/1.2373 Å, and 1.3963/1.3879, 1.4207/1.4325 Å, respectively. In the literature, the, N-N, C=O, N=C, bond lengths are calculated as 1.404, 1.212, 1.280 Å [28, 29], respectively. The calculated structural parameters for triazole rings in the titled molecule are in a proper settlement with the literature outcomes [32, 33]. Forms the optimized molecular structure; no arithmetical in molecule changes have been observed. The theoretical results of the titled molecule show that the optimized bond lengths and angles are mildly higher than the experimental value because the theoretical computations are in gas phase isolated molecule and the experimental results are in the liquid molecule. Thus, the changes of the geometric properties are not possible. The Mulliken atomic charge parameters in gas phase of the compound (**1**) are listed in (Table 3 and Figure 2) [34]. While all electronegative oxygen (O), nitrogen (N) atoms have negative atomic charge values and all hydrogen atoms of the title compound have positive atomic charge values. The carbon atoms surrounded with electronegative atoms (N, O) have positive atomic charge values for titled compound. The C2 atom surrrounded with three electronegative atoms (N, N, O) and C1 atom which is surrounded two electronegative atoms (N, N) with have the highest positive charges values (Table 3).

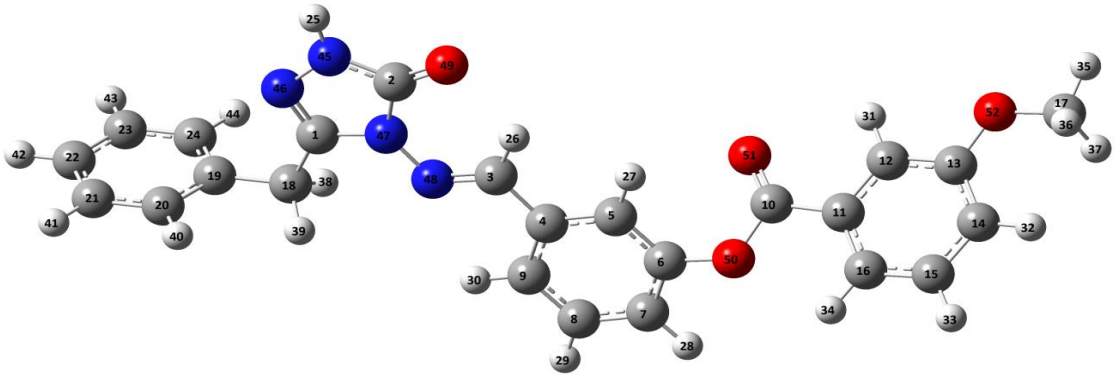

Figure 1. The optimized molecular structure of titled compound

Table 1. The calculated bond angles (^{0}) of titled compound

	Bond Angles (^{0})	HF 6-311G(d)	B3LYP 6-311G(d)	HF 3-21G	B3LYP 3-21G
1	C1-N46-N45	105.085	104.762	104.151	103.303
2	C1-N47-N48	121.201	121.375	120.504	120.764
3	C1-N47-C2	108.064	108.228	109.237	109.263
4	C1-C18-H38	107.913	108.167	107.954	108.152
5	C1-C18-H39	107.908	108.196	107.955	108.155
6	H38-C18-H39	105.622	105.118	106.600	106.330
7	N46-N45-H25	120.708	120.193	119.984	119.339
8	N46-N45-C2	113.844	114.566	112.948	114.063
9	N46-C1-C18	126.879	126.347	127.323	126.418
10	H25-N45-C2	125.449	125.240	127.068	126.598
11	N45-C2-N47	101.790	101.058	102.051	101.152
12	N45-C2-O49	129.588	130.153	130.266	130.918
13	O49-C2-N47	128.622	128.788	127.683	127.930
14	C2-N47-N48	130.732	130.393	130.260	129.973
15	N47-C1-C18	121.904	122.267	121.064	121.364
16	H38-C18-C19	110.609	110.583	110.757	110.663
17	H39-C18-C19	110.609	110.587	110.757	110.666
18	C18-C19-C20	120.619	120.674	120.453	120.479
19	C18-C19-C24	120.610	120.615	120.456	120.483
20	C19-C20-H40	119.716	119.565	119.656	119.497
21	C19-C24-H44	119.719	119.544	119.658	119.498
22	C19-C20-C21	120.724	120.749	120.539	120.551
23	H40-C20-C21	119.560	119.686	119.805	119.952
24	C20-C21-C22	120.099	120.083	120.079	120.078
25	C20-C21-H41	119.785	119.804	119.824	119.847
26	H41-C21-C22	120.116	120.113	120.097	120.075
27	C21-C22-C23	119.586	119.622	119.675	119.705
28	C21-C22-H42	120.207	120.191	120.162	120.148
29	H42-C22-C23	120.207	120.187	120.163	120.148
30	C22-C23-C24	120.101	120.087	120.079	120.077
31	C22-C23-H43	120.118	120.108	120.098	120.076
32	H43-C23-C24	119.781	119.805	119.824	119.847
33	C23-C24-C19	120.722	120.748	120.539	120.551
34	C23-C24-H44	119.559	119.708	119.803	119.951
35	H44-C24-C19	119.719	119.544	119.658	119.498
36	N47-N48-C3	120.057	119.251	119.102	117.273
37	N48-C3-H26	122.326	121.998	122.492	122.376
38	N48-C3-C4	120.421	120.236	120.074	119.717
39	H26-C3-C4	117.253	117.766	117.434	117.907
40	C3-C4-C5	118.014	117.940	117.813	117.991

41	C3-C4-C9	122.587	122.494	121.661	121.660
42	C4-C5-H27	120.986	120.230	120.934	121.055
43	C4-C5-C6	119.885	119.577	119.061	119.184
44	H27-C5-C6	119.128	120.188	120.005	119.761
45	C5-C6-O50	117.960	122.301	124.883	125.403
46	C5-C6-C7	121.119	121.035	120.819	120.641
47	O50-C6-C7	120.838	116.553	114.298	113.956
48	C6-C7-H28	120.044	119.246	118.720	118.565
49	C6-C7-C8	118.953	119.278	119.697	119.803
50	H28-C7-C8	121.002	121.476	121.583	121.632
51	C7-C8-H29	119.433	119.482	119.589	119.510
52	C7-C8-C9	120.703	120.521	120.326	120.352
53	H29-C8-C9	119.864	119.997	120.085	120.137
54	C8-C9-H30	120.489	120.821	121.104	121.533
55	C8-C9-C4	119.940	120.021	119.571	119.671
56	H30-C9-C4	119.571	119.157	119.325	118.796
57	C9-C4-C5	119.399	119.566	120.526	120.348
58	C6-O50-C10	119.998	120.544	128.246	125.487
59	O50-C10-O51	123.386	123.559	123.478	124.173
60	O50-C10-C11	111.903	111.224	111.450	110.214
61	O51-C10-C11	124.711	125.217	125.072	125.613
52	C10-C11-C16	122.174	122.643	122.033	122.596
63	C10-C11-C12	117.240	117.005	116.966	116.566
64	C11-C12-H31	120.465	120.160	120.619	120.127
65	C11-C12-C13	120.285	120.316	120.061	120.243
66	H31-C12-C13	119.251	119.524	119.320	119.629
67	C12-C13-O52	115.788	115.708	116.044	115.819
68	C12-C13-C14	119.428	119.518	119.360	119.186
69	C13-O52-C17	119.946	118.628	120.963	118.215
70	O52-C13-C14	124.785	124.774	124.596	124.995
71	O52-C17-H35	106.189	105.751	105.464	104.862
72	O52-C17-H36	111.459	111.527	111.308	111.608
73	O52-C17-H37	111.465	111.541	111.308	111.608
74	H35-C17-H37	109.100	109.241	109.618	109.682
75	H35-C17-C36	109.105	109.254	109.618	109.682
76	H36-C17-C37	109.431	109.429	109.446	109.306
77	C13-C14-C15	119.786	119.690	120.128	120.133
78	H32-C14-C15	119.099	119.315	119.176	119.236
79	C14-C15-H33	119.033	119.057	119.259	119.178
80	H33-C15-C16	119.835	119.817	119.946	119.917
81	C15-C16-H34	120.744	120.876	121.399	121.681
82	C15-C16-C11	118.784	118.998	118.655	118.695
83	C16-C11-C12	120.586	120.352	121.001	120.838
84	H34-C16-C11	120.472	120.126	119.946	119.624
85	C16-C11-C12	120.586	120.352	121.001	120.838
86	C13-C14-H32	121.116	120.995	120.696	120.631

Table 2. The calculated bond lenghts (A^0) of titled compound

	Bond Lenghts (A^0)	**HF 6-311G(d)**	**HF 3-21G**	**B3LYP 6-311G(d)**	**B3LYP 3-21G**
1	C1-N46	1.2772	1.2651	1.2946	1.3110
2	C1-N47	1.3846	1.3818	1.3906	1.3905
3	C1-C18	1.4937	1.4988	1.4982	1.4971
4	C18-H38	1.0837	1.0839	1.0950	1.0969
5	C18-H39	1.0837	1.0839	1.0949	1.0970
6	C18-C19	1.5136	1.5122	1.5128	1.5172
7	C19-C20	1.3855	1.3873	1.3966	1.3994
8	C20-H40	1.0728	1.0762	1.0863	1.0848
9	C20-C21	1.3833	1.3843	1.3927	1.3957
10	C21-H41	1.0720	1.0754	1.0855	1.0840
11	C21-C22	1.3837	1.3845	1.3931	1.3967
12	C22-H42	1.0719	1.0753	1.0853	1.0838
13	C22-C23	1.3837	1.3845	1.3933	1.3966
14	C23-H43	1.0720	1.0754	1.0855	1.0840
15	C23-C24	1.3833	1.3843	1.3924	1.3958
16	C24-H44	1.0728	1.0762	1.0863	1.0848
17	C24-C19	1.3855	1.3872	1.3969	1.3994
18	N46-N45	1.4272	1.3634	1.3789	1.4387
19	N45-H25	0.9919	0.9886	1.0054	1.0087
20	N45-C2	1.3539	1.3458	1.3684	1.3774
21	C2-O49	1.2187	1.1961	1.2156	1.2373
22	N47-C2	1.3963	1.3879	1.4207	1.4325
23	N47-N48	1.3980	1.3628	1.3690	1.4097
24	N48-C3	1.2669	1.2573	1.2847	1.2973
25	C3-H26	1.0701	1.0740	1.0866	1.0848
26	C3-C4	1.4715	1.4767	1.4663	1.4651
27	C4-C5	1.3884	1.3876	1.4004	1.4034
28	C4-C9	1.3866	1.3920	1.4039	1.4036
29	C5-H27	1.0657	1.0748	1.0824	1.0778
30	C5-C6	1.3807	1.3797	1.3905	1.3948
31	C6-O50	1.3956	1.3786	1.3936	1.4098
32	C6-C7	1.3815	1.3767	1.3892	1.3974
33	C7-H28	1.0694	1.0736	1.0840	1.0816
34	C7-C8	1.3817	1.3872	1.3957	1.3439
35	C8-H29	1.0712	1.0747	1.0849	1.0834
36	C8-C9	1.3811	1.3799	1.3868	1.3917
37	C9-H30	1.0695	1.0726	1.0803	1.0819
38	O50-C10	1.3573	1.3400	1.3734	1.3941
39	C10-O51	1.2048	1.1782	1.2019	1.2276
40	C10-C11	1.4787	1.4921	1.4891	1.4807
41	C11-C16	1.3884	1.3933	1.4026	1.4028
42	C11-C12	1.3772	1.3802	1.3926	1.3923
43	C12-H31	1.0687	1.0722	1.0829	1.0812
44	C12-C13	1.3859	1.3902	1.3972	1.3998
45	C13-O52	1.3689	1.3455	1.3611	1.3824
46	C13-C14	1.3821	1.3851	1.3987	1.3998
47	C14-H32	1.0695	1.0726	1.0827	1.0815
48	C14-C15	1.3879	1.3902	1.3966	1.3990
49	C15-H33	1.0715	1.0750	1.0851	1.0836
50	C15-C16	1.3769	1.3770	1.3873	1.3902
51	C16-H34	1.0673	1.0713	1.0815	1.0794
52	O52-C17	1.4368	1.3977	1.4193	1.4603
53	C17-H35	1.0772	1.0785	1.0882	1.0899
54	C17-H36	1.0831	1.0849	1.0954	1.0968
55	C17-H37	1.0831	1.0850	1.0952	1.0968

Table 3. The Mulliken atomic charges of titled compound

	HF 6-311G(d)	HF 3-21G	B3LYP 6-311G(d)	B3LYP 3-21G
C1	0.569	0.816	0.450	0.678
C2	0.782	1.250	0.583	0.941
C3	0.036	0.195	-0.053	0.110
C4	-0.043	-0.164	-0.023	-0.056
C5	-0.271	-0.246	-0.208	-0.212
C6	0.328	0.383	0.231	0.301
C7	-0.211	-0.254	-0.193	-0.192
C8	-0.208	-0.227	-0.202	-0.183
C9	-0.194	-0.205	-0.159	-0.173
C10	0.647	1.008	0.430	0.708
C11	-0.204	-0.246	-0.157	-0.107
C12	-0.241	-0.199	-0.203	-0.166
C13	0.368	0.417	0.272	0.322
C14	-0.300	-0.267	-0.259	-0.207
C15	-0.195	-0.227	-0.193	-0.182
C16	-0.211	-0.209	-0.160	-0.183
C17	-0.416	-0.273	-0.464	-0.336
C18	-0.587	-0.504	-0.589	-0.514
C19	0.071	-0.032	0.081	0.047
C20	-0.227	-0.213	-0.189	-0.176
C21	-0.203	-0.231	-0.192	-0.182
C22	-0.224	-0.241	-0.188	-0.186
C23	-0.203	-0.231	-0.193	-0.182
C24	-0.227	-0.213	-0.186	-0.176
H25	0.407	0.405	0.372	0.354
H26	0.306	0.331	0.261	0.263
H27	0.240	0.324	0.229	0.247
H29	0.228	0.252	0.201	0.196
H28	0.238	0.266	0.209	0.206
H30	0.243	0.271	0.211	0.207
H31	0.264	0.305	0.230	0.230
H32	0.242	0.255	0.216	0.196
H33	0.224	0.251	0.199	0.195
H34	0.244	0.274	0.213	0.206
H35	0.233	0.239	0.233	0.227
H36	0.208	0.200	0.211	0.199
H37	0.207	0.200	0.211	0.199
H38	0.266	0.270	0.249	0.240
H39	0.265	0.270	0.248	0.240
H40	0.212	0.239	0.187	0.184
H41	0.218	0.241	0.192	0.187
H42	0.217	0.241	0.192	0.186
H43	0.218	0.241	0.192	0.187
H44	0.213	0.239	0.188	0.184
N45	-0.592	-0.761	-0.497	-0.593
N46	-0.247	-0.383	-0.186	-0.334
N47	-0.478	-0.855	-0.373	-0.629
N48	-0.273	-0.362	-0.205	-0.322
O49	-0.532	-0.671	-0.389	-0.520
O50	-0.510	-0.815	-0.373	-0.600
O51	-0.436	-0.616	-0.317	-0.480
O52	-0.461	-0.735	-0.336	-0.550

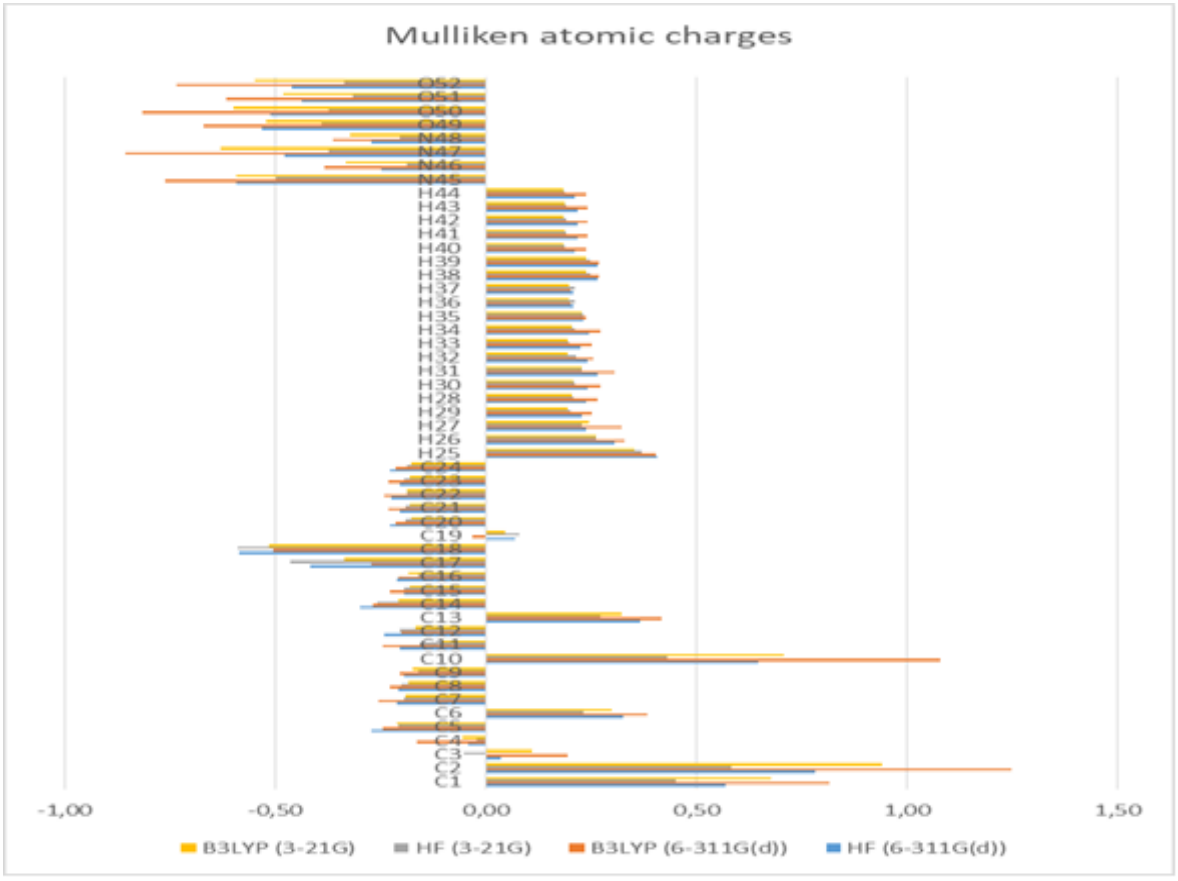

Figure 2. The Mulliken atomic charges graphs of titled compound

B. FT-IR Spectral Analysis

3-Benzyl-4-[3-(3-methoxybenzoxy)-benzylidenamino]-4,5-dihydro-1*H*-1,2,4-triazol-5-one have 52 atoms. All vibration frequency modes of the title compound are 150. The observed vibrational frequencies of the title compound are given by using same basis sets and methods (Table 4-5 and Figure 3). These effective basic frequencies have been allocated were distributed as 101 in-plane and 49 out-of-plane vibration modes.

N-H vibrations

The NH stretching mode of the title molecule is detected at 3167 cm^{-1}. The band is computed at 3656 (DFT/6-311G(d)), 3770 (HF/6-311G(d)), 3515 (DFT/3-21G)) and 3540 (HF/3-21G) cm^{-1}. The NH in-plane bending mode causes the absorption band at 1356 cm^{-1} in IR spectrum. The NH in-plane bending mode causes the absorption band at 1356 cm^{-1}. The band is identified as 1463 (DFT/6-311G(d)), 1390 (HF/6-311G(d)) and 1418 (DFT/3-21G) and 1390 (HF/3-21G) cm^{-1} for the NH in-plane bending mode. The out-of-plane bending mode of N-H is also observed at 432 (exp.) and 453 (DFT/6-311G(d)), 478 (HF/6-311G(d)), 553 (DFT/3-21G) and 582 (HF/3-21G) cm^{-1}.

C-H vibrations

In IR spectra, the C-H stretching vibration mode for sp^2 hybrid carbon atoms leads to absorption band over 3000 cm^{-1} [35]. The C-H stretching vibration modes in aromatic rings of the title compound may be allocated to the bands detected at 3027 cm^{-1}. The band is computed at 3039 (DFT/6-311G(d)), 3086 (HF/6-311G(d)), 3043 (DFT/3-21G)) and 3076 (HF/3-21G) cm^{-1}. The C-H stretching vibration band in the aliphatic group is observed at 2968 cm^{-1} (exp.) and 3014 (DFT/6-311G(d)), 3064 (HF/6-311G(d)), 2983 (DFT/3-21G)) and 2968 (HF/3-21G) cm^{-1}. The methylene group's scissoring mode is attributed at 1420 cm^{-1} (exp.) and 1343 (DFT/6-311G(d)), 1409 (HF/6-311G(d)), 1362 (DFT/3-21G) and 1385 (HF/3-21G) cm^{-1}.

CC vibrations

The CC stretching modes in aromatic ring are noted at 1489 cm^{-1} (exp.) and 1343 (DFT/6-311G(d)), 1377 (HF/6-311G(d)), 1309 (DFT/3-21G)) and 1334 (HF/3-21G) cm^{-1}. In addition, these stretching modes can be applied in combination with other vibrational bands under 1400 cm^{-1}. Other experimental and calculated vibrational bands of the title molecule are presented in Table 4 and 5.

CO vibrations

In the carbonyl and carboxyl groups, C=O stretching mode offers a strong absorption band in 1900-1500 cm^{-1} region [35]. Depending on the impact, like the electronic and mass impacts of the surrounding substituents, physical state, inter/intramolecular hydrogen bonding and conjugation, the location of this stretching band may be altered. The C=O stretching frequencies are found the strong bands in 1730 and 1698 (exp.) cm^{-1}, 1792 and 1787 (DFT/6-311G(d)), 1903 and 1883 (HF/6-311G(d)), 1709 and 1675 (DFT/3-21G)), 1744 and 1732 (HF/3-21G) cm^{-1}. In FT-IR spectrum, the C-O stretching vibration mode is determined in 1350-1200 cm^{-1} areas [35]. In this regard, the C-O stretching band is observed at 1273 (exp.) cm^{-1} and 1306 (DFT/6-311G(d)), 1326 (HF/6-311G(d)), 1287 (DFT/3-21G) and 1294 (HF/3-21G) cm^{-1} in FT-IR spectrum.

CN, NN vibrations

The C=N stretching modes in triazole ring are observed at 1578 cm^{-1} computing at 1273 (exp.) cm^{-1} and 1306 (DFT/6-311G(d)), 1326 (HF/6-311G(d)), 1287 (DFT/3-21G)) and 1294 (HF/3-21G) cm^{-1}. The NN stretching modes in triazole group is observed at 1048 cm^{-1} and calculated as 1087 (DFT/6-311G(d)), 1129 (HF/6-311G(d)), 1117 (DFT/3-21G)) and 1128 (HF/3-21G). The NN stretching vibration mode is found at 1214 (exp.) cm^{-1} and computed as 1255 (DFT/6-311G(d)), 1277 (HF/6-311G(d)), 1255 (DFT/3-21G) and 1256 (HF/3-21G) cm^{-1} with another mixed band. Another calculated vibrational modes for the title molecule are given ın Table 4 and 5.

Table 4. The calculated IR frequencies of titled compound (cm^{-1}) (6-311G(d))

	Vibrational Frequencies (PED%)	**HF**	**B3LYP**
1	τ CNNC(28), τ COCC(23), τ NCCC(19), τ CCCN(18)	6	8
2	τ CCCC(11), τ COCC(28), τ CCOC(21)	7	15
3	τ CCOC(30)	16	17
4	τ NNNC(13)	18	21
5	τ CNNC(16), τ CCCC(18), τ NCCC(11)	34	33
6	τ CNNC(14), τ CCCC(19), τ NCCC(13)	34	34
7	δ COC(10), τ CCNN(12), τ CCCC(13)	46	42
8	τ CCCC(12)	57	56
9	τ CCNN(23), δ COC(15), τ CCCN(10)	64	65
10	δ CCN(12), δ CCC(10), τ CCCC(22)	70	82
11	τ HCOC(10), τ CCCC(12), τ COCC(59), δ CCN(13), δ CCC(12)	84	83
12	δ CCO(11), τ CNNC(12), τ NNCC(13), τ NCCC(10), τ CCCN(11)	107	110
13	τ NNCC(12), δ NCC(13)	131	117
14	δ CNN(14), τ NNCC(13),τ NCNC(11), τ NCCC(11)	155	155
15	τ CCCC(16)	164	170
16	δ NCC(15), τ CCCC(21)	179	182
17	ν CC(10), δ NCN(14)	196	191
18	τ HCOC(18), τ CCCC(24), τ COCC(10), τ OCCC(19), τ CCCN(15)	223	214
19	τ CCCN(32)	224	216
20	τ CCCN(43), τ NNCC(19), τ HCOC(19), τ CCCC(29)	226	236
21	ν CC(11), τ CCCC(15)	246	237
22	δ COC(22), τ CCCN(19), τ HCOC(41), δ COC(12)	268	262
23	τ HCOC(41), τ CCCC(27), τ HNNC(26)	281	279
24	τ HNNC(20), τ CNNC(35), τ NNCC(15), τ HCOC(41), τ CCCC(24)	293	281
25	δ COC(23), δ OCO(13)	307	295
26	δ COC(10)	320	317
27	δ CCC(31), τ HCCC(13)	346	333
28	τ CCCN(10), τ CCNN(32), τ COCC(10)	361	348
29	δ OCN(13), δ NCN(12), δ CNN(10), δ NNC(13), δ COC(10)	404	381
30	τ HCCC(17), τ CCCC(80)	431	411
31	δ CCC(26), δ COC(11)	439	426
32	τ CCCC(10)	459	439
33	δ CCO(10), δ CCC(12), τ HNNC(53)	461	449
34	τ HNNC(40),τ NCNC(11)	478	453
35	τ HNNC(20), τ HCCC(12), τ CCCN(12)	485	462

36	τ HCCC(12), τ CCCC(20)	500	478
37	δ CCC(16), δ COC(12)	504	492
38	τ HCCC(11), τ CCCC(13), τ OCCC(36), δ OCN(11), δ CCC(18)	579	551
39	δ CCC(24), δ OCN(15), δ COC(12)	581	561
40	δ CCC(18), δ COC(18)	583	567
41	δ CCO(12)	600	584
42	δ CCC(17), δ CNN(12)	615	595
43	τ CCCN(19), τ COCC(11), τ CCOC(13), δ OCO(10)	628	599
44	δ CCC(17), δ OCN(18)	647	629
45	δ CCC(17), δ OCN(20), δ CCN(10)	651	632
46	τ HNNC(12), τ NNCC(12),τ NCNC(39), τ HCCC(14)	688	655
47	τ HCCC(24), τ CCCC(17), δ CCC(21)	705	683
48	ν CC(12), δ CCC(22)	716	684
49	τ HCCC(36), τ COCC(10), τ CCOC(19)	721	692
50	τ CCCC(43), τ HCCC(27), τ CCCN(18)	725	698
51	τ HCCC(48)	741	706
52	τ ONNC(80), τ HCCC(10)	778	738
53	τ HCCC(14)	808	751
54	τ HCCC(13), τ OCOC(42)	812	753
55	δ CNN(12)	814	786
56	τ HCCC(26)	831	789
57	ν CC(11), δ CNN(15), ν NC(11)	833	798
58	τ HCCC(50), τ OCOC(25)	860	802
59	δ OCO(11), τ HCCC(14)	861	815
60	τ HCCC(28)	873	835
61	ν NN(10), δ CCN(13)	889	839
62	ν NN(12), δ NCN(14), δ CCN(13), τ HCCC(99)	898	849
63	ν OC(11), τ HCCC(11)	926	876
64	τ HCCC(39), τ CCCC(10)	966	891
65	ν OC(12), τ HCCC(24)	967	896
66	τ HCCC(29), ν CC(10), δ HCC(30)	969	914
67	τ HCCC(17)	980	917
68	τ HCCC(31)	982	918
69	δ HCC(32), τ HCCC(31), δ NNC(34)	985	928
70	τ HCCC(84), τ CCCC(12)	995	947
71	ν CC(11), δ CCC(13)	1027	956
72	τ HCCC(22), τ CCCC(13)	1031	961
73	τ HCCC(58), ν CC(45), δ CCC(49)	1034	967
74	τ HCCC(36), τ CCCC(26), ν CC(19), δ CCC(39)	1035	977
75	ν CC(28), δ CCC(30), τ HCCC(22)	1044	1002
76	τ HCNN(88), τ HCCC(57)	1049	1005
77	ν CC(37), δ CCC(22), δ HCC(20)	1053	1007
78	ν CC(41), δ CCC(51), δ HCC(20)	1068	1011
79	δ NNC(34), τ HCNN(87)	1082	1026
80	ν CC(35), δ HCC(23), δ CCC(10)	1089	1044
81	ν OC(61), ν CC(40), δ HCC(25)	1113	1062
82	ν OC(10), δ HCC(19), δ CCC(12)	1126	1085
83	ν NC(12), ν NN(38)	1129	1087
84	ν CC(43), δ HCC(25), ν OC(12)	1138	1097
85	ν CC(33), δ HCC(20)	1142	1098
86	ν CC(31), δ HCC(16)	1144	1110
87	ν CC(16), δ HCC(32)	1150	1163
88	δ HCH(25), τ HCOC(22), ν NC(10), ν NN(28), δ HNN(10)	1158	1171
89	ν CC(21), δ HCC(36), τ HCCC(12)	1168	1175
90	ν CC(11), δ HCC(40)	1211	1180
91	ν CC(10), δ HCC(17)	1232	1185
92	ν CC(23), δ HCC(70), δ HCH(25), τ HCOC(26)	1232	1197
93	δ HCH(13), τ HCOC(23)	1242	1199
94	ν NC(13), ν NN(17), δ OCN(10), ν CC(19), δ HCC(10), τ HCCC(10)	1250	1204
95	ν CC(11), δ HCC(41), τ HCCC(26), τ HCOC(11)	1251	1208
96	ν CC(20), δ HCC(14), τ HCCC(12)	1261	1215
97	ν OC(10), ν CC(12), δ HCC(12)	1267	1223
98	ν NC(10), ν NN(13), δ CNN(14)	1277	1255
99	ν NN(11), τ HCCC(12), ν CC(13), δ HCC(38)	1301	1275
100	ν CC(11), ν OC(16)	1313	1285
101	δ HCC(24), ν OC(43), ν CC(12)	1326	1306
102	δ HCC(24), ν NC(10), δ CNN(15), τ HCCC(24)	1350	1311
103	δ HCC(12), τ HCCC(18), ν OC(18)	1368	1321
104	ν CC(53), δ HCC(23)	1373	1331
105	ν CC(62), δ HCC(41)	1377	1343
106	ν CC(56), δ HCC(17)	1409	1350
107	δ HCC(73), ν NC(11), ν NN(16), δ CNN(16), τ HCCC(13)	1411	1355
108	ν NC(10), δ HNN(26), δ HCN(24), τ HCCC(16)	1463	1390
109	δ HNN(47), δ HCN(16), ν OC(13)	1484	1401

110	ν CC(10), ν NC(12)	1506	1438
111	ν CC(12), δ HCN(13), δ HCC(14)	1525	1460
112	ν CC(22), δ HCC(10), δ HCH(11)	1533	1465
113	δ HCH(85)	1534	1476
114	ν CC(12), δ HCC(25), δ HCN(16), δ HCH(12), τ HCCC(16)	1541	1479
115	δ HCH(57)	1546	1480
116	δ HCH(72), τ HCOC(13)	1562	1498
117	δ HCH(64), τ HCOC(11)	1570	1509
118	δ HCC(37), δ HCH(17), δ CCC(11), ν CC(65)	1574	1511
119	δ HCC(11), δ CCC(11)	1577	1515
120	δ HCC(60), δ CCC(13), ν CC(10)	1583	1524
121	ν NC(10), ν CC(27), δ HCC(10), δ CCC(10)	1690	1609
122	ν CC(15), δ CCC(18)	1691	1610
123	ν CC(30), δ CCC(12), δ HCC(11)	1696	1619
124	ν NC(23), ν CC(18), δ HCC(10)	1716	1628
125	ν NC(22), ν CC(16)	1717	1632
126	ν CC(65), δ HCC(10)	1719	1638
127	ν CC(46), δ HCC(18), ν NC(42)	1772	1641
128	ν NC(45), ν CC(10)	1801	1653
129	ν OC(85), ν NC(12)	1863	1787
130	ν OC(71), ν NC(11)	1903	1792
131	ν CH(91)	3030	2982
132	ν CH(100)	3064	3014
133	ν CH(100)	3086	3039
134	ν CH(58)	3093	3039
135	ν CH(46)	3149	3116
136	ν CH(84)	3166	3126
137	ν CH(91)	3170	3128
138	ν CH(28)	3181	3138
139	ν CH(50)	3188	3139
140	ν CH(54)	3190	3145
141	ν CH(12)	3191	3146
142	ν CH(91)	3199	3148
143	ν CH(50)	3202	3159
144	ν CH(48)	3216	3168
145	ν CH(27)	3218	3177
146	ν CH(40)	3220	3180
147	ν CH(25)	3226	3184
148	ν CH(40)	3236	3185
149	ν CH(48)	3239	3195
150	ν NH(100)	3770	3656

*ν, stretching; δ, bending; τ, torsion

Table 5. The calculated IR frequencies of titled compound (cm^{-1}) (3-21G)

	Vibrational Frequencies (PED%)	HF	B3LYP
1	τ CNNC(15), τ NCNC(17), τ CCCN(19)	7	7
2	τ CCCC(68)	10	16
3	τ CCOC(25), τ COCC(49), τ CCCC(10)	17	19
4	δ CCC(14), δ CNN(18), δ CCN(21), δ COC(15)	22	22
5	τ NCNC(23), τ CCCC(34), τ CCOC(22)	25	25
6	τ CNNC(10), τ CCCC(13), τ CCOC(16), τ CCCN(16), τ NCNC(11)	32	34
7	δ NCC(14), δ COC(20), τ CCCC(13)	48	48
8	τ CCNN(41), τ COCC(25)	63	63
9	τ HCOC(11), τ COCC(55), τ CCNN(12)	67	78
10	δ CNN(11), δ CCN(12), δ CCC(11), τ CCCC(22)	82	80
11	τ CCCC(22), τ COCC(26)	87	94
12	δ CCC(11), δ CCO(16)	101	100
13	τ CNNC(23), τ CCCN(13), τ NCNC(14), τ NNCC(22)	121	121
14	τ CCNN(11), τ CCCC(14), τ CNNC(15), τ CCCN(17)	168	163
15	τ CCCN(31), τ CCCC(20),τ CNNC(11)	178	175
16	δ CNN(11), CC(10), δ COC(11)	183	184
17	δ NCC(17), δ CCN(10), δ COC(29)	199	200
18	τ HCOC(44), τ CCCC(13), τ COCC(10), τ OCCC(18)	210	208
19	δ CNN(11)	212	210
20	ν CC(14), δ CCC(10), τ CCCC(16)	240	235
21	τ CCCN(36), τ CCCC(12), τ CCNN(16)	262	258
22	δ COC(40)	266	267
23	τ HCOC(19), τ CCCC(30), τ OCCC(11)	273	269
24	τ CNNC(14), τ CCCN(27), τ CCNN(25), τ CCCC(17), τ OCCC(10)	280	286
25	δ OCO(12), δ COC(22)	316	316
26	δ CCC(21), τ NCNC(23)	327	316
27	δ CCC(12), τ HCCC(17), τ NNCC(16), τ NCNC(18)	343	328
28	τ CCCN(10), τ CCNN(29), δ OCO(13), δ COC(16)	361	354
29	δ OCO(15), δ OCN(10), τ CCNN(29), τ NNCC(15)	370	355
30	δ OCN(14), δ CCC(11), τ HCCC(18), τ CCCC(80)	420	409
31	δ OCN(16), τ HCCC(19), τ CCCC(79)	425	413
32	δ CCC(27), δ COC(11)	437	433
33	τ CCCC(48)	464	446
34	τ HCCC(21), τ CCCN(19), τ CCOC(16), τ CCCC(17)	484	467
35	ν CC(10), τ HCCC(20), τ CCCC(27), τ OCCC(10)	485	469
36	δ CCC(13), τ CCCC(10)	494	485
37	τ HNNC(89), δ CCC(17), δ COC(18)	557	540
38	δ OCN(17), δ CCC(11), δ NNC(14)	559	548
39	τ HCCC(12), τ CCCC(16), τ OCOC(13), τ OCCC(32)	572	551
40	δ CCC(12), δ COC(21), τ HNNC(95), τ NCNC (10)	582	553
41	δ CCC(18), δ CCO(11)	589	579
42	δ CCC(11), δ CCO(10)	597	587
43	δ OCN(14), δ CCC(11), τ CCCN(19), τ COCC(19), τ CCOC(18)	626	609
44	δ CCC(15), δ OCN(13), τ CCCN(16), τ OCCC(18)	637	613
45	δ CCC(49), τ NCNC(22)	648	636
46	δ CCC(14), τ NNCC(14), τ NCNC(43), τ CCNN(14)	668	641
47	ν CC(12), δ CCC(31)	694	683
48	τ HCCC(15), τ CCCC(21)	705	689
49	τ HCCC(31), τ CCCC(18)	727	702
50	τ HCCC(31), τ CCCC(31)	732	706
51	τ HCCC(42), τ COCC(10), τ CCOC(15), τ CCCN(15)	737	710
52	ν NN(10), τ HCCC(19)	742	725
53	τ ONNC(78), ν NC(14), δ NCC(12), δ CNN(29)	768	733
54	τ HCCC(13), τ OCOC(54)	784	744
55	ν NC(13), δ NCN(19), δ NCC(12), δ OCO(25)	792	753
56	ν CC(10), ν OC(12), δ OCO(28), τ ONNC(75)	793	771
57	ν CC(20)	798	781
58	δ CCN(23), δ CNN(11)	821	801
59	τ HCCC(26), τ CCOC(15), τ CCCC(10)	845	809
60	τ HCCC(57), τ CCCC(10), τ OCOC(10)	861	811
61	ν CC(10), τ HCCC(63)	865	819
62	ν CC(13), ν OC(20), τ HCCC(99)	877	838
63	ν CC(11), ν OC(18), τ HCCC(99)	897	857
64	ν CC(13), δ HCC(35), τ HCCC(30)	933	909
65	δ HCC(33), τ NCNC(12), τ HCCC(31)	934	913
66	δ NCC(33), τ HCCC(44)	970	920
67	δ NCC(12), τ HCCC(48)	993	924
68	ν CC(11), δ CCC(11), τ HCCC(31)	995	925
69	τ HCCC(28), τ CCCC(13)	997	944
70	ν CC(41), δ CCC(13), δ NCN(15), δ NCC(39)	1002	949
71	ν CC(62), ν CCC(12), τ HCCC(83), τ CCCC(14)	1007	967

72	ν CC(17), ν CCC(25), τ HCCC(26), τ CCOC(12)	1011	978
73	ν CC(51), ν OC(20), τ HCCC(34), δ HCC(20)	1017	985
74	ν NC(31), δ CNN(11)	1036	988
75	δ CCC(49), δ HCC(10), τ HCCC(55)	1040	994
76	τ HCCC(45), τ HCNN(13)	1041	995
77	ν CC(17), δ CCC(10), τ HCCC(82), τ CCCC(17)	1048	997
78	ν OC(56), ν CC(17), δ CCC(10), τ HCCC(19), τ CCCC(17)	1050	998
79	ν CC(52), δ CCC(23), τ HCCC(62)	1074	1005
80	ν OC(35), δ CCC(14), τ HCCC(47)	1078	1012
81	δ CCC(41), δ HCC(18), τ HCCC(30), τ CCCC(29)	1079	1029
82	ν CC(50), δ HCC(19), τ HCNN(84)	1085	1046
83	ν OC(12), ν CC(15), δ CCC(11), δ HCC(18)	1090	1069
84	ν CC(51), δ HCC(20)	1099	1080
85	ν CC(36), δ HCC(19)	1100	1086
86	ν CC(32), δ HCC(20), τ HCNN(75)	1106	1091
87	ν CC(62), ν NC(26), ν NN(15)	1128	1117
88	ν CC(13), δ HCH(23), τ HCOC(26)	1142	1118
89	ν NC(10), ν OC(12), δ HCC(12), δ HCH(24), τ HCOC(26)	1155	1137
90	ν CC(19), δ HCH(24), τ HCOC(28)	1156	1149
91	ν OC(12), δ HCC(15)	1159	1172
92	ν NC(10), ν NN(11), δ HCC(23), δ NNC(10)	1171	1181
93	ν CC(23), δ HCC(36), τ HCOC(24), δ HCH(13)	1184	1188
94	ν CC(23), δ HCC(36), δ CCC(15)	1199	1188
95	ν CC(17), δ CCC(12), δ HCC(65)	1212	1194
96	ν CC(12), δ HCC(65), τ HCCC (10)	1214	1201
97	ν CC(33), δ HCC(44), τ HCCC(24)	1218	1201
98	ν OC(10), ν CC(14), δ HCC(40), τ HCCC(24)	1219	1202
99	ν CC(14), ν OC(12), δ HCC(14)	1245	1237
100	ν CC(12), ν OC(10), ν NN(12), ν NC(13), δ NNC(18)	1256	1255
101	ν CC(15), ν NC(12), δ HCN(11), δ HCC(38), τ HCCC(15)	1267	1268
102	ν OC(23), ν CC(53), δ HCC(14)	1276	1285
103	ν CC(32), ν OC(23), δ HCC(10), τ HCCC(10)	1294	1287
104	ν CC(33), ν NC(12), ν NN(10), δ HCN(11), δ HCC(13), τ HCCC(27)	1310	1294
105	ν CC(46), δ HCC(40)	1334	1309
106	δ HNN(79), δ HCC(74)	1352	1317
107	δ HCC(74), δ HNN(77)	1354	1324
108	ν CC(10), δ HCN(31), δ HCC(69), τ HCCC(27)	1382	1352
109	δ HCC(70), δ HCN(22), τ HCCC(37)	1385	1362
110	ν NC(11), δ HCN(29)	1418	1390
111	ν CC(17), δ HCN(17), δ HCC(11)	1453	1418
112	ν CC(30), δ HCC(15)	1458	1432
113	δ HCC(10), δ HCH(89)	1476	1452
114	ν CC(28), δ HCC(30), δ HCH(86)	1480	1458
115	ν CC(10), δ HCC(30), δ HCH(72)	1483	1460
116	δ HCC(46)	1508	1482
117	ν CC(20), δ HCC(25)	1513	1483
118	δ HCC(68), δ CCC(10)	1521	1498
119	δ HCH(76), τ HCOC(11)	1525	1502
120	δ HCH(74)	1534	1514
121	ν NC(54), ν CC(27), δ CCC(10), δ HCC(11)	1596	1531
122	ν NC(49), ν CC(21), δ HCC(10), δ CCC(10)	1598	1543
123	ν CC(29), δ HCC(16), δ CCC(13)	1600	1557
124	ν CC(28), δ HCC(20), δ CCC(12)	1613	1564
125	ν CC(45), δ HCC(25)	1617	1567
126	ν NC(11), ν CC(28), δ CCC(10), δ HCC(10)	1623	1572
127	ν CC(47), δ HCC(23), ν NC(39)	1635	1581
128	ν CC(62), δ HCC(11), ν NC(45)	1671	1585
129	ν OC(85), δ CNN(12)	1732	1675
130	ν OC(85)	1744	1709
131	ν CH(91)	2907	2923
132	ν CH(100)	2936	2956
133	ν CH(50)	2956	2976
134	ν CH(100)	2968	2985
135	ν CH(46)	3016	3050
136	ν CH(85)	3041	3074
137	ν CH(92)	3043	3076
138	ν CH(48)	3053	3076
139	ν CH(51)	3061	3086
140	ν CH(52)	3062	3092
141	ν CH(36)	3063	3094
142	ν CH(52)	3075	3095
143	ν CH(51)	3080	3107
144	ν CH(68)	3090	3120
145	ν CH(67)	3092	3122

146	ν CH(30)	3097	3126
147	ν CH(56)	3108	3134
148	ν CH(48)	3119	3150
149	ν CH(50)	3138	3168
150	ν NH(100)	3540	3515

*ν, stretching; δ, bending; τ, torsion

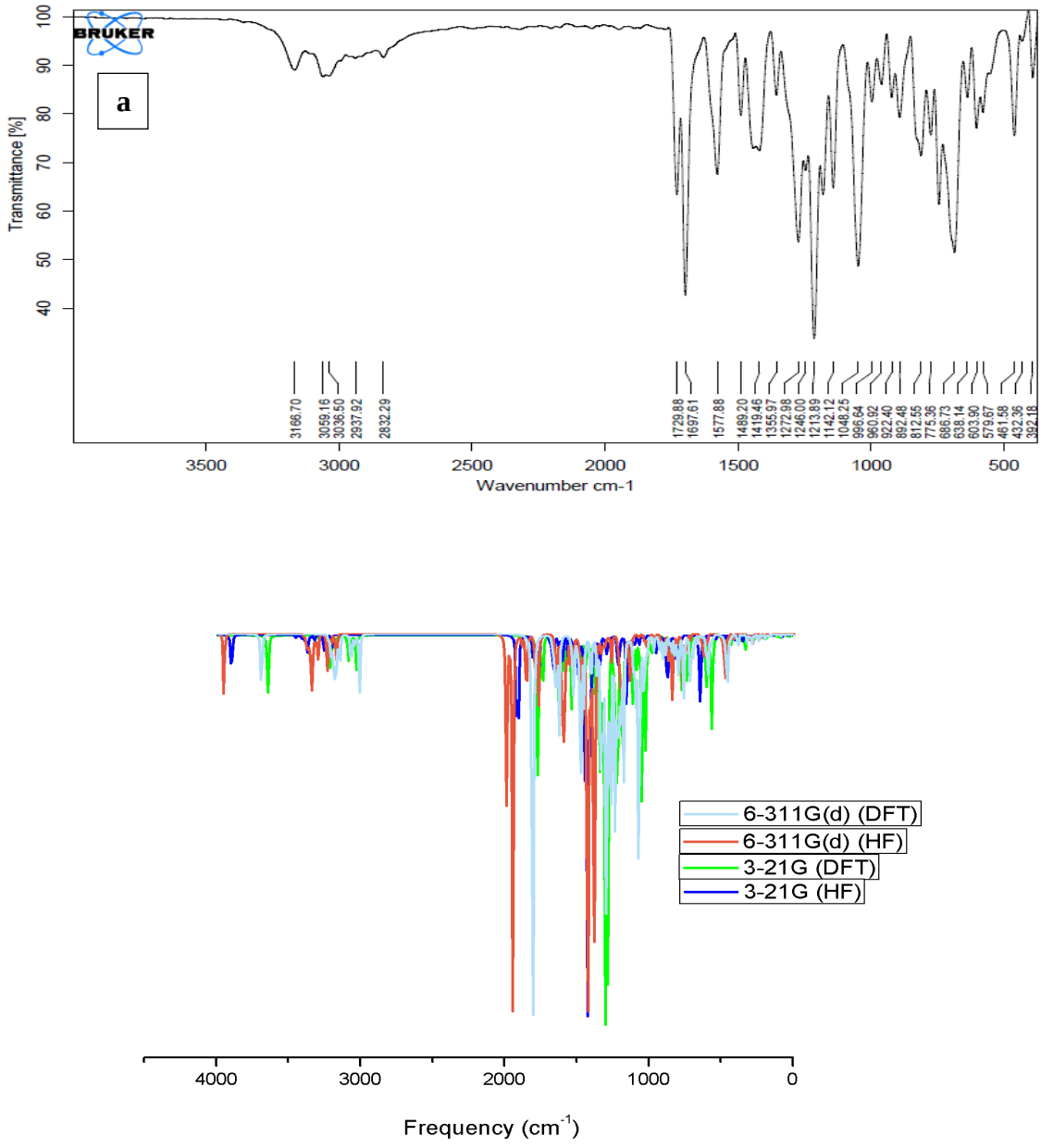

Figure 3. The calculated FT-IR spectrums of titled compound (Experimental (a), 6-311G(d), 3-21G HF/B3LYP)

C. ^{13}C and ^{1}H NMR Chemical Shift and Regression Analyses

The ^{1}H and ^{13}C NMR chemical shifts values (in DMSO solvent and in gas phase) of the compound (**1**) have been performed with the DFT (B3LYP) and Hartree Fock (HF) methods and 6-311G(d) and 3-21G basis sets (Figure 4). The ^{1}H and ^{13}C-NMR chemical shift values of titled compound were listed in Table 6 and 7. The experimental ^{1}H and ^{13}C-NMR resonance signals had been compared with calculated chemical shift values**.** At

155-185 ppm, the carbons in carboxyl groups produce resonance signals [36]. The ^{13}C NMR chemical shift signal of the carbon (C10) in carboxyl groups is at 164.32 ppm, computing 151.08/166.49 (HF/DFT 6-311G(d)) ppm in vaccuum, 152.89/168.05 (HF/DFT 6-311G(d)) ppm in DMSO, 128.38/133.09 (HF/DFT 3-21G) ppm in vaccuum and 129.23/133.77 (HF/DFT 3-21G) ppm in DMSO. The resonance signal will be provided at 159.46 ppm by the C13, which is linked to the electronegative oxygen atom whereas it are found as 149.52/165.17 (HF/DFT 6-311G(d)) ppm in vaccuum, 149.42/165.40 (HF/DFT 6-311G(d)) ppm in DMSO, 115.69/124.07 (HF/DFT 3-21G) ppm in vaccuum and 115.40/124.17 (HF/DFT 3-21G) ppm in DMSO. Similarly, the resonance signal will be provided at 152.46 ppm by the C6, which is linked to the electronegative oxygen atom whereas it are found as 142.06/157.75 (HF/DFT 6-311G(d)) ppm in vaccuum, 141.29/157.38 (HF/DFT 6-311G(d)) ppm in DMSO, 111.05/120.81 (HF/DFT 3-21G) ppm in vaccuum and 110.93/120.91 (HF/DFT 3-21G) ppm in DMSO. The NMR signals are also reported at 146.25 ppm and 151.17 ppm for C1 and C2 atoms linked to electronegative nitrogen and oxygen atoms. The NMR signals are also reported at 146.25 ppm and 151.17 ppm for C1 and C2 atoms linked to electronegative nitrogen and oxygen atoms. For the C1 and C2 carbon atoms, calculated NMR chemical shift values are 141.28/151.69 (HF/DFT 6-311G(d)) ppm in vaccuum, 143.73/151.69 (HF/DFT 6-311G(d)) ppm in DMSO, 113.73/116.46 (HF/DFT 3-21G) ppm in vaccuum and 115.60/116.46 (HF/DFT 3-21G) ppm in DMSO. The ^{13}C-NMR signals for carbon atom (C3) in azomethine group are noted as 151.02 ppm (exp.) and 142.16/152.35 (HF/DFT 6-311G(d)) ppm in vaccuum, 142.84/152.82 (HF/DFT 6-311G(d)) ppm in DMSO, 115.19/117.33 (HF/DFT 3-21G) ppm in vaccuum and 115.55/117.55 (HF/DFT 3-21G) ppm in DMSO. The ^{13}C-NMR signals for carbon atoms in aromatic rings are noted as the 114.29-135.76 ppm and calculated at the interval 110-150 ppm. The carbon-13 resonance signal of the saturated C17 atom (sp^3 hybridized) having a bond with electronegative atom (O52) are observed at 55.48 (exp.) ppm and 35.38/53.54 (HF/DFT 6-311G(d)) ppm in vaccuum, 35.76/54.10 (HF/DFT 6-311G(d)) ppm in DMSO, 15.66/31.38 (HF/DFT 3-21G) ppm in vaccuum and 16.17/32.03 (HF/DFT 3-21G) ppm in DMSO. The proton resonace signals of H35, H36 and H37 hydrogen atoms in methoxy group are found at 3.88 ppm, whereas calculated at the interval 3.70-2.70 ppm. The proton chemical shift signal of the N-H in trizole ring are observed at 12.02 ppm and it is computed as 5.37/6.18 (HF/DFT 6-311G(d)) ppm in vaccuum, 5.81/6.67 (HF/DFT 6-311G(d)) ppm in DMSO, 4.49/5.47 (HF/DFT 3-21G) ppm in vaccuum and 4.93/5.99 (HF/DFT 3-21G) ppm in DMSO. The ^{1}H-NMR chemical shift signals of phenyl rings are found at the interval 7.21-7.80 ppm and computed at the interval 6.50-8.00 ppm. Furthermore, the methylene H38 and H39 protons are noted as 4.08 ppm (exp.) and found at the interval 2.05-3.65 ppm. The proton resonance signal for hydrogen atom (H25) in azomethine group is noted as 9.74 (exp.) ppm and 9.02/9.60 (HF/DFT 6-311G(d)) ppm in vaccuum, 9.00/9.55 (HF/DFT 6-311G(d)) ppm in DMSO, 4.49/5.47 (HF/DFT 3-21G) ppm in vaccuum and 4.93/5.99 (HF/DFT 3-21G) ppm in DMSO.

The outcomes indicated a properly correlation R^2 between calculated ^{1}H and ^{13}C-NMR chemical shifts ratios and experimental ones [22]. The calculated R^2 (6-311G(d)/3-21G) have been 0.9963/0.99886 (gas phase), 0.9974/0.9888 (DMSO) for ^{13}C-NMR chemical shifts values and 0.6498/0.6176 (gas phase), 0.6933/0.6753 (DMSO) for ^{1}H-NMR chemical shifts values. The experimental and calculated between ^{1}H and ^{13}C NMR chemical shifts values of titled compound were found a linear correlation whereas the calculated R^2 for ^{1}H-NMR chemical shifts ratios are decrease than ^{13}C-NMR chemical shifts ratios due to the fact N45-H25 proton of 4,5-dihydro-1*H*-1,2,4-triazol-5-one ring used to be revealed the acidic character.

Table 6. The ^{1}H and ^{13}C NMR isotropic chemical shifts of titled compound (with respect to TMS, all values in ppm) (6-311G(d)).

	$\delta_{Exp.}$	$\delta_{cal.}$ B3LYP (Vacum)	$\delta_{cal.}$ B3LYP (DMSO)	Different	Different (DMSO)	$\delta_{cal.}$ HF(Vacum)	$\delta_{cal.}$ HF (DMSO)	Different	Different (DMSO)
C1	146.25	151.69	153.58	-5.44	-7.33	141.28	143.73	4.97	2.52
C2	151.17	152.49	153.47	-1.32	-2.30	141.75	142.67	9.42	8.50
C3	151.02	152.35	152.82	-1.33	-1.80	142.16	142.84	8.86	8.18
C4	135.27	139.99	139.47	-4.72	-4.20	126.69	126.44	8.58	8.83
C5	125.83	130.20	129.52	-4.37	-3.69	117.92	118.37	7.91	7.46
C6	152.46	157.75	157.38	-5.29	-4.92	142.06	141.29	10.40	11.17
C7	124.86	125.86	127.23	-1.00	-2.37	118.70	118.93	6.16	5.93
C8	130.10	131.62	133.13	-1.52	-3.03	120.41	121.16	9.69	8.94
C9	120.23	123.51	123.99	-3.28	-3.76	114.22	114.92	6.01	5.31
C10	164.32	166.49	168.05	-2.17	-3.73	151.08	152.89	13.24	11.43
C11	130.26	134.84	133.84	-4.58	-3.58	122.87	121.82	7.39	8.44
C12	122.14	124.78	122.87	-2.64	-0.73	115.21	113.25	6.93	8.89
C13	159.46	165.17	165.40	-5.71	-5.94	149.52	149.42	9.94	10.04
C14	114.39	115.00	117.83	-0.61	-3.44	103.99	106.57	10.40	7.82
C15	130.23	131.62	133.26	-1.39	-3.03	120.81	122.37	9.42	7.86
C16	120.38	124.19	124.31	-3.81	-3.93	113.43	113.72	6.95	6.66
C17	55.48	53.54	54.10	1.94	1.38	35.28	35.76	20.20	19.72

C18	31.11	35.35	34.80	-4.24	-3.69	18.00	17.56	13.11	13.55
C19	135.76	138.91	139.56	-3.15	-3.80	126.51	127.14	9.25	8.62
C20	128.83	133.59	133.78	-4.76	-4.95	122.37	122.48	6.46	6.35
C21	128.38	130.87	131.43	-2.49	-3.05	120.19	120.59	8.19	7.79
C22	126.68	129.82	130.31	-3.14	-3.63	118.96	119.27	7.72	7.41
C23	128.38	130.92	131.42	-2.54	-3.04	120.24	120.60	8.14	7.78
C24	128.83	133.70	133.81	-4.87	-4.98	122.41	122.49	6.42	6.34
H25	12.02	6.18	6.67	5.84	5.35	5.37	5.81	6.65	6.21
H26	9.74	9.60	9.55	0.14	0.19	9.02	9.00	0.72	0.74
H27	7.66	7.14	7.18	0.52	0.48	6.67	6.88	0.99	0.78
H28	7.47	6.80	7.05	0.67	0.42	6.66	6.86	0.81	0.61
H29	7.61	7.11	7.38	0.50	0.23	6.86	7.12	0.75	0.49
H30	7.80	7.79	7.91	0.01	-0.11	7.61	7.76	0.19	0.04
H31	7.75	7.53	7.35	0.22	0.40	7.44	7.25	0.31	0.50
H32	7.36	6.35	6.74	1.01	0.62	6.06	6.48	1.30	0.88
H33	7.57	7.04	7.31	0.53	0.26	6.79	7.09	0.78	0.48
H34	7.73	7.47	7.57	0.26	0.16	7.20	7.33	0.53	0.40
H35	3.88	3.70	3.79	0.18	0.09	3.08	3.15	0.80	0.73
H36	3.88	3.21	3.38	0.67	0.50	2.51	2.71	1.37	1.17
H37	3.88	3.21	3.39	0.67	0.49	2.52	2.72	1.36	1.16
H38	4.08	3.62	3.77	0.46	0.31	2.99	3.18	1.09	0.90
H39	4.08	3.65	3.78	0.43	0.30	2.98	3.16	1.10	0.92
H40	7.28	6.98	7.16	0.30	0.12	6.69	6.90	0.59	0.38
H41	7.32	7.05	7.23	0.27	0.09	6.76	6.96	0.56	0.36
H42	7.22	6.98	7.16	0.24	0.06	6.7	6.89	0.52	0.33
H43	7.32	7.05	7.23	0.27	0.09	6.76	6.95	0.56	0.37
H44	7.28	6.98	7.16	0.30	0.12	6.70	6.90	0.58	0.38

Table 7. The ^{1}H and ^{13}C NMR isotropic chemical shifts of titled compund (with respect to TMS, all values in ppm 3-21G)).

	$\delta_{Exp.}$	$\delta_{cal.}$ B3LYP (Vacum)	$\delta_{cal.}$ B3LYP (DMSO)	Different	Different (DMSO)	$\delta_{cal.}$ HF(Vacum)	$\delta_{cal.}$ HF (DMSO)	Different	Different (DMSO)
C1	146.25	116.46	117.68	29.79	28.57	113.73	115.60	32.52	30.65
C2	151.17	115.56	115.98	35.61	35.19	114.90	115.34	36.27	35.83
C3	151.02	117.33	117.55	33.69	33.47	115.19	115.55	35.83	35.47
C4	135.27	100.69	100.01	34.58	35.26	93.41	92.63	41.86	42.64
C5	125.83	90.33	89.66	35.50	36.17	84.15	83.46	41.68	42.37
C6	152.46	120.81	120.81	31.65	31.65	111.05	110.93	41.41	41.53
C7	124.86	87.83	88.90	37.03	35.96	83.53	84.56	41.33	40.30
C8	130.10	93.51	94.78	36.59	35.32	88.76	90.02	41.34	40.08
C9	120.23	87.30	87.58	32.93	32.65	82.98	83.42	37.25	36.81
C10	164.32	133.09	133.77	31.23	30.55	128.38	129.23	35.94	35.09
C11	130.26	96.61	95.77	33.65	34.49	90.29	89.36	39.97	40.90
C12	122.14	88.37	86.86	33.77	35.28	85.48	83.68	36.66	38.46
C13	159.46	124.07	124.19	35.39	35.27	115.69	115.40	43.77	44.06
C14	114.39	82.99	85.10	31.40	29.29	78.12	80.33	36.27	34.06
C15	130.23	94.35	95.67	35.88	34.56	88.90	90.44	41.33	39.79
C16	120.38	88.19	88.22	32.19	32.16	83.98	84.43	36.40	35.95
C17	55.48	31.38	32.03	24.10	23.45	15.66	16.17	39.82	39.31
C18	31.11	14.19	13.75	16.92	17.36	-0.44	-0.78	31.55	31.89
C19	135.76	99.03	99.47	36.73	36.29	92.50	92.95	43.26	42.81
C20	128.83	96.26	96.29	32.57	32.54	91.05	91.12	37.78	37.71
C21	128.38	93.59	93.98	34.79	34.40	88.87	89.23	39.51	39.15
C22	126.68	92.91	93.32	33.77	33.36	88.07	88.45	38.61	38.23
C23	128.38	93.59	93.99	34.79	34.39	88.86	89.23	39.52	39.15
C24	128.83	96.25	96.29	32.58	32.54	91.05	91.12	37.78	37.71
H25	12.02	5.47	5.99	6.55	6.03	4.49	4.93	7.53	7.09
H26	9.74	9.37	9.30	0.37	0.44	8.82	8.73	0.92	1.01
H27	7.66	7.76	7.66	-0.10	0.00	7.37	7.25	0.29	0.41
H28	7.47	5.73	6.03	1.74	1.44	5.70	6.04	1.77	1.43
H29	7.61	6.05	6.39	1.56	1.22	5.87	6.25	1.74	1.36
H30	7.80	6.88	7.01	0.92	0.79	6.79	6.97	1.01	0.83
H31	7.75	6.69	6.50	1.06	1.25	6.82	6.57	0.93	1.18

H32	7.36	5.22	5.67	2.14	1.69	4.93	5.44	2.43	1.92
H33	7.57	5.98	6.30	1.59	1.27	5.74	6.13	1.83	1.44
H34	7.73	6.63	6.77	1.10	0.96	6.49	6.70	1.24	1.03
H35	3.88	3.38	3.52	0.50	0.36	2.72	2.82	1.16	1.06
H36	3.88	2.72	2.97	1.16	0.91	1.74	2.03	2.14	1.85
H37	3.88	2.72	2.97	1.16	0.91	1.74	2.03	2.14	1.85
H38	4.08	2.85	3.02	1.23	1.06	2.05	2.28	2.03	1.80
H39	4.08	2.84	3.02	1.24	1.06	2.05	2.28	2.03	1.80
H40	7.28	5.98	6.20	1.30	1.08	5.72	5.98	1.56	1.30
H41	7.32	5.96	6.19	1.36	1.13	5.69	5.94	1.63	1.38
H42	7.22	5.90	6.13	1.32	1.09	5.64	5.89	1.58	1.33
H43	7.32	5.96	6.19	1.36	1.13	5.69	5.94	1.63	1.38
H44	7.28	5.98	6.20	1.30	1.08	5.72	5.98	1.56	1.30

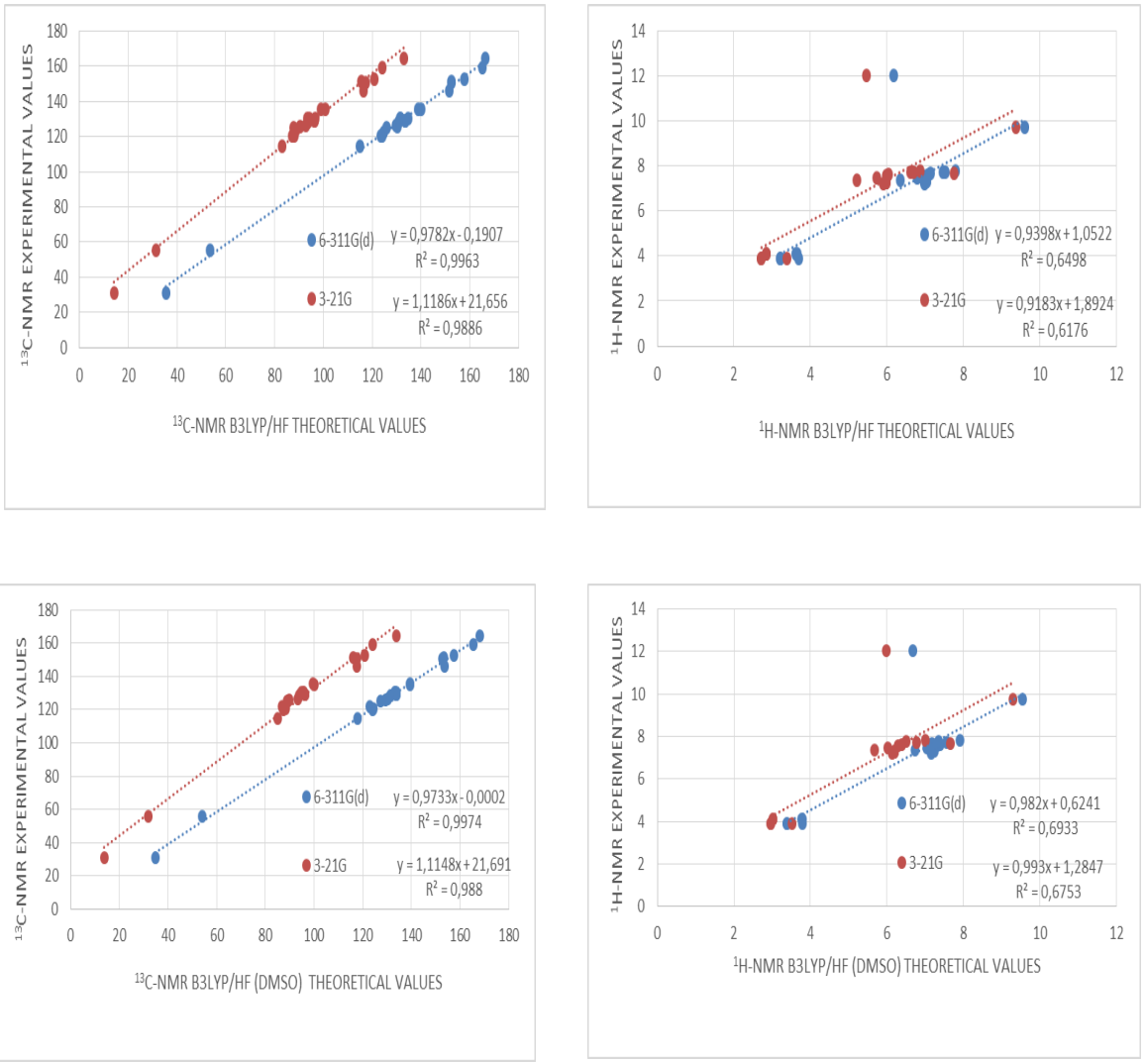

Figure 4. Compared values of calculated and experimental ^{13}C- and ^{1}H-NMR chemical shifts values of titled compound with 6-311G(d) and 3-21G/B3LYP and HF (gas phase/DMSO).

D. UV-vis. Spectral Values

The oscillator strengths (*f*), absorption wavelengths (λ) and excitation energies of UV–Vis electron absorption spectroscopy (in ethanol solvent) of the titled compound have been performed using B3LYP/HF strategies with 6-311G(d) and 3-21G basis sets and introduced in Figure 5 [31]. The absorption wavelengths exhibited at 296, 246 and 222 nm have been determined to n→π*, π→π* and n→σ* transitions. The UV-vis. spectrums, wavelengths, oscillator strengths and excitation energies of the title compound are performed through use of TD-DFT and TD-HF methods (in the ethanol solvent) (Figure 5). Seen from Figure 5, for the title compound, the most intense absorption peak has been determined as 314.66 nm/3.9402 eV/0.3808 (DFT/6-311G(d)) and 311.142 nm/3.9813 eV/0.3140 (DFT/3-21G) in ethanol solvent (wavelength/excitation energy/oscillator strength).

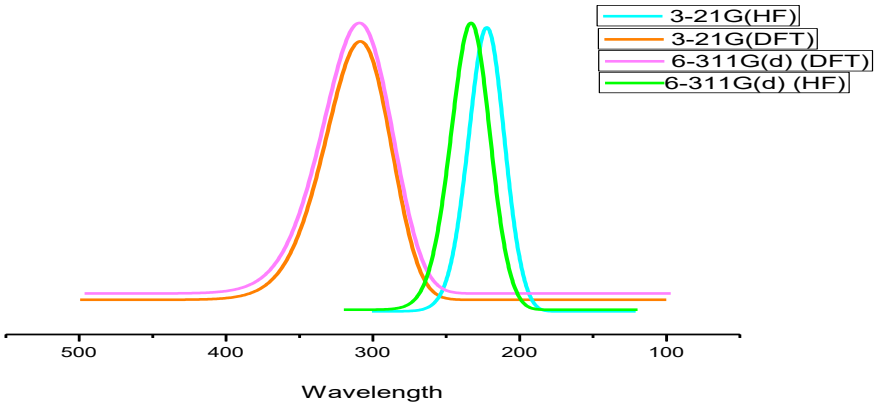

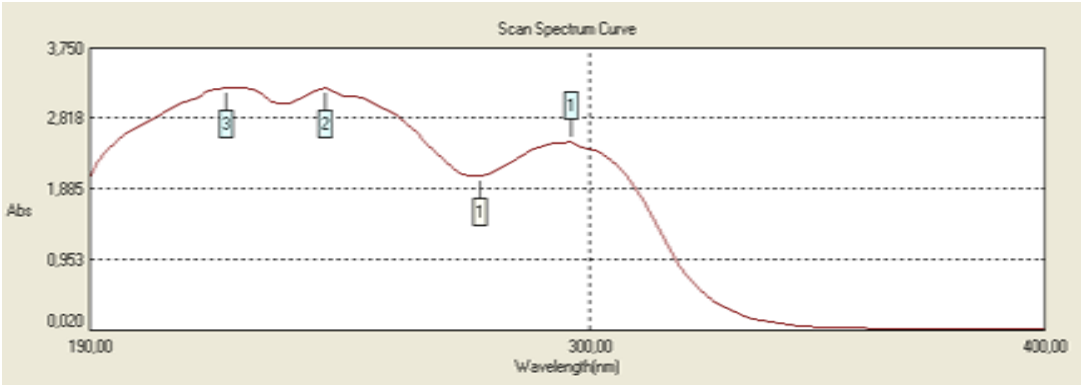

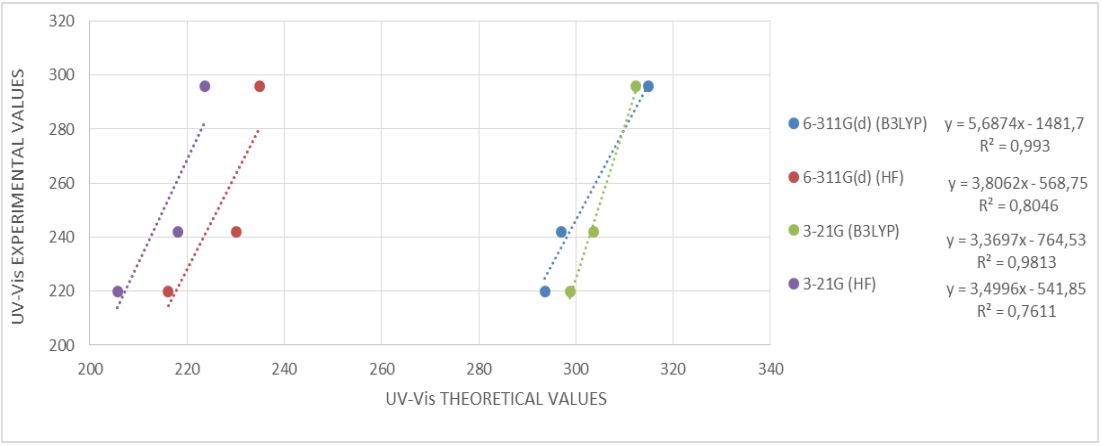

Experimental (nm)	λ (nm) HF/B3LYP 6-311G(d)	λ (nm) HF/B3LYP 3-21G	Excitation Energy (eV) HF/B3LYP 6-311G(d)	Excitation Energy (eV) HF/B3LYP 3-21G	*f* (osillatör strengths) HF/B3LYP 6-311G(d)	*f* (osillatör strengths) HF/B3LYP 3-21G
296.00	234.95/314.66	223.50/311.142	5.2771/3.9402	5.5475/3.9813	0.5996/0.3808	0.5346/0.3140
246.00	230.09/303.75	218.28/304.07	5.3885/4.0818	5.6799/4.0775	1.1098/0.0506	0.2134/0.0912
222.00	216.16/294.10	205.74/297.98	5.7356/4.2157	6.0262/4.1608	0.0933/0.0463	0.1106/0.0861

Figure 5. The absorption wavelength (λ), oscillator strengths (*f*), excitation energies and UV-vis spectrums and graphs (B3LYP/HF 6-311G(d), 3-21G) of the title compound

D. HOMO-LUMO Analyses, Electronic and Thermodynamic Properties

The highest occupied molecular orbital (HOMO) and the lowest unoccupied molecular orbital (LUMO), are referred to as the frontier molecular orbitals (FMOs) and are the major orbitals participating with chemical reactions [37]. The HOMO describes the external most orbital filled by electrons. This is directly related to the ionization potential of the molecule. It can be considered a valance band of the system since it is an electron donor. The LUMO indicates the first empty orbital that is unfilled with electrons. It has a direct connection to the electron affinity. It can be regarded as a conductive band of the system as an electron acceptor. The energy gaps between HOMO and LUMO indicate molecular chemical stabilization and is very crucial in determining molecular electrical characteristics [38]. The highest occupied molecular orbital (HOMO) and the lowest unoccupied molecular orbital (LUMO) of titled compound have been simulated and determined. The molecular electrostatic potential (MEP), HOMO and LUMO energies and their 3D plots of this compound were observed both two methods and basis sets (Table 8 and Figure 6). Applying HOMO-LUMO energies, the quantum molecular descriptors such as energy gap (ΔE), electron affinity (A) electronegativity (χ), global softness (σ)/hardness (η), ionization potential (I) were found [39].

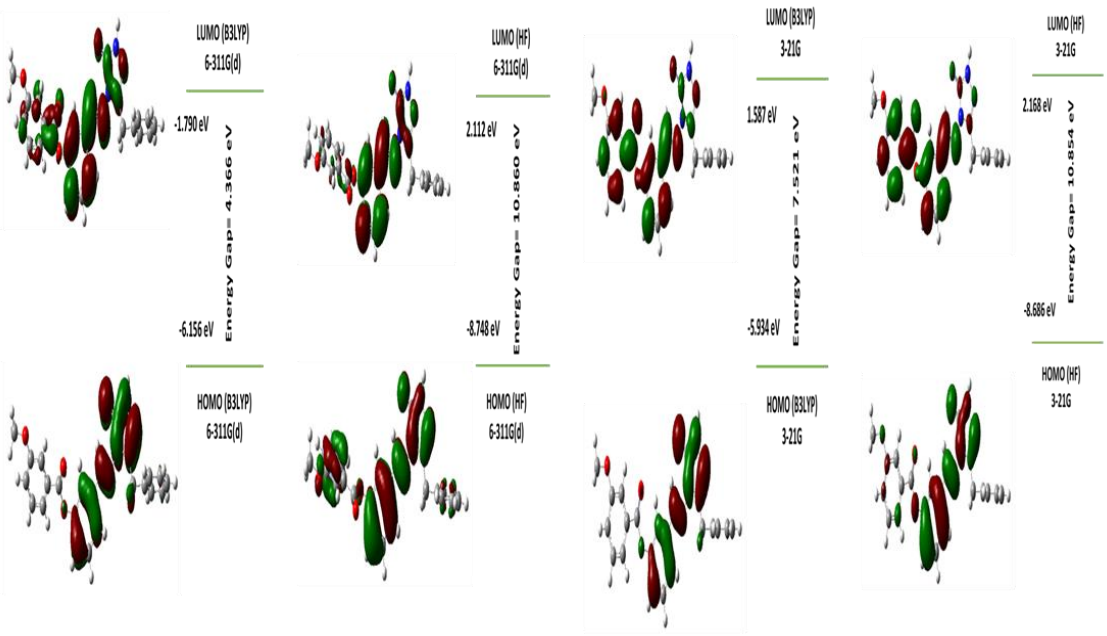

Figure 6. 3D plots of HOMO and LUMO energies of titled compound at the HF/B3LYP 6-311G(d) and 3-21G basis sets

Table 8. Electronic structure parameters of titled compound

	HF/B3LYP 6-311G(d)	**HF/B3LYP 3-21G**
E_{HOMO} (eV)	-8.748/-6.156	-8.686/-5.934
E_{LUMO} (eV)	2.112/-1.790	2.168/1.587
$\Delta E = E_{LUMO}-E_{HOMO}$ (eV)	10.860/4.366	10.854/7.521
I (eV)	8.748/6.156	8.686/5.934
A(eV)	-2.112/1.790	-2.168/-1.587
χ (eV)	3.318/3.973	3.259/2.173
η (eV)	5.430/2.183	5.427/3.760
S (eV^{-1})	136.360/339.159	136.429/196.901

Table 11 shows that the certain thermodynamic parameters (such as rotational temperatures thermal energy, rotational constants, zero-point vibrational energies (ZPVE), heat capacity and entropy) without experimental determinations for the title molecule were found through use of B3LYP and HF method and 6-311G(d) and 3-21G basis sets. For molecular rotation, vibration and translation at 298.15 K, thermal energy (E) was computed as the total amount of zero point energy and thermal energy corrections. The addition of RT to the thermal energy and electronic energy acquired enthalpy at 1 atm and 298.15 K. The total entropy as shown in Table 11 were observed as 192.405/149.140 (B3LYP/HF 6-311G(d)), 192.022/186.593 (B3LYP/HF 3-21) Cal/Mol-Kelvin. Furthermore, the ZPVE were found as 254.335/271.399 (B3LYP/HF 6-311G(d)), 254.484/274.108 (B3LYP/HF 3-21) KCal/Mol. These findings are essential for testing our outcomes' accuracy. In view of the results of energy, ZPVE, entropy and dipole moment, the compound can be used for the new synthesis.

Table 9. The calculated dipole moment of titled compound (6-311G(d) HF/B3LYP, 3-21G HF/B3LYP)

Dipole Moment	**HF 6-311G(d)**	**HF 3-21G**	**B3LYP 6-311G(d)**	**B3LYP 3-21G**
μ_x	1.5107	1.0617	1.0629	1.3160
μ_y	5.4894	5.1789	3.7320	2.9717
μ_z	1.8427	1.8765	1.4287	1.3859
μ_{Toplam}	5.9842	5.6098	4.1351	3.5332

Table 10. The calculated total energy values of titled compound

Energy	**HF 6-311G(d)**	**HF 3-21G**	**B3LYP 6-311G(d)**	**B3LYP 3-21G**
(a.u.)	-1438.000	-1429.684	-1446.803	-1438.506

Table 11. The thermodynamic parameters of titled compound

Parameters	**B3LYP 6-311G(d)**	**HF 6-311G(d)**	**B3LYP 3-21G**	**HF 3-21G**
Zero-point vibrational energy (Kcal/mol)	254.335	271.399	254.484	274.108
Thermal Energy E (KCal/Mol)				
Translational	0.889	0.889	0.889	0.889
Rotational	0.889	0.889	0.889	0.889
Vibrational	267.852	213.844	215.138	288.177
Total	269.630	215.621	216.915	289.954
Rotational temperatures (Kelvin)				
A	0.40972	0.02076	0.02058	0.02096
B	0.03544	0.00166	0.00168	0.00170
C	0.03364	0.00160	0.00157	0.00159
Rotational constants (GHZ)				
A	0.92675	0.43261	0.42889	0.43684
B	0.11905	0.03456	0.03502	0.03542
C	0.10765	0.03332	0.03276	0.03315
Thermal Capacity CV (Cal/Mol-Kelvin)				
Translational	2.981	2.981	2.981	2.981

Rotational	2.981	2.981	2.981	2.981
Vibrational	98.979	68.198	97.304	88.932
Total	104.941	74.160	103.266	94.894
Entropy S (Cal/Mol-Kelvin)				
Translational	44.053	42.713	44.053	44.053
Rotational	37.729	34.537	37.772	37.681
Vibrational	113.624	71.889	110.247	104.860
Total	195.405	149.140	192.022	186.593
Zero-point correction (Hartree/Particle)	0.4021	0.4325	0.4055	0.4368
Thermal correction to Gibbs Free Energy	0.3378	0.3684	0.3422	0.4368
Thermal correction to Energy	0.4297	0.4585	0.4335	0.4621
Sum of electronic and zero-point Energies	-1446.401	-1437.567	-1438.101	-1429.247
Thermal correction to Enthalpy	0.4306	0.4595	0.3422	0.4630
Sum of electronic and thermal Energies	-1446.373	-1437.541	-1438.074	-1429.222
Sum of electronic and thermal Enthalpies	14666.372	-1437.540	-1438.073	-1429.221
Sum of electronic and thermal Free Energies	-1446.465	-1437.631	-1438.164	-1429.310

The MEP is related to the electronic density and very beneficial descriptor for figuring out sites for electrophilic and nucleophilic reactions. The MEP at B3LYP/HF 6-311G(d) and 3-21G strategies optimized geometry was once performed and proven in Figure **7**. As viewed from Figure **7** the most high positive area is N-H located on hydrogen atom while the most high negative area is positioned on electronegative oxygen atoms and nitrogen atom (N46, O49, O51, O52) inside the molecule which can be regarded as possible site electrophilic attack.

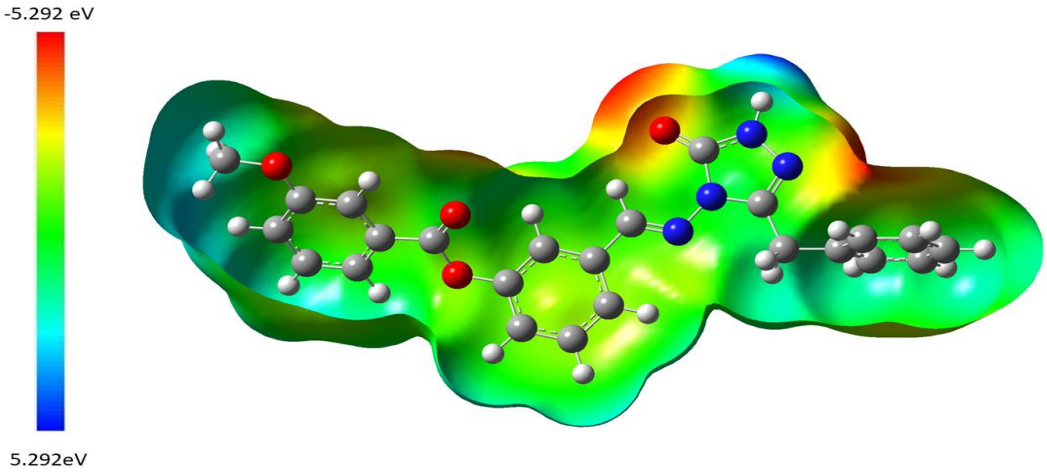

Figure 5. The molecular surface map of titled compound

VI. CONCLUSION

The 3-benzyl-4-[3-(3-methoxybenzoxy)-benzylidenamino]-4,5-dihydro-1*H*-1,2,4-triazol-5-one molecule was synthesized and spectroscopically characterized through experimental techniques such as FT-IR, NMR and UV-vis spectroscopies. The experimental spectral findings were supported by DFT/HF and 6-311G(d) and 3-21G quantum chemistry calculation methods. In the experimental FT-IR spectrum, the board band in the area of 2700-3500 cm^{-1} and also occuring resonance signal at 12.02 ppm in experimental proton-NMR spectrum indicates that the title molecule was synthesized. The findings of PED output acquired from the coordinate analysis were clearly allocated to the different modes of vibrations. Furthermore, there is a proper settlement

between experimental values and calculated vibrational frequencies. The comprehensive information on the compound (**1**) was obtained when comparing the experimental and measured spectroscopic values. There was a nice consensus with optimized structural parameters (bond angles (˚) and bond lengths (Å)) of the title molecule. The TD-DFT and TD-HF calculations (in ethanol solvent) were provided a close settlement with experimental absorption spectral values. The most reactive locations occurring both electrophilic and nucleophilic attack was determined through MEP. The most negative area is localized over the nitrogen and oxygen atom of triazole ring and the most positive region is localized over the N-H group, indicating a possible site for nucleophilic attack. The calculated ^{1}H and ^{13}C-NMR chemical shifts had been performed with experimental values in gas phase and in DMSO solvent and displaying a very excellent agreement. The thermodynamic properties of titled molecule are broadly used analyzing the reaction mechanisms of natural compounds. These results are important to test the precision of our results. In the light of the energy, ZPVE, entropy and dipole moment results, this molecule can be applied for the new synthesis. HOMO energy is recognized as the capacity of the molecule to give electrons (π_{donor}), the potential of the LUMO electricity molecule to accept electrons ($\pi_{Acceptor}$). Many information about quantum molecular descriptors determining the chemical reactivity of the title molecule was obtained from the HOMO-LUMO energies. The DFT/B3LYP method and 6-311G(d) basis set were demonstrated excellent outcomes for general performance of the title molecule.

REFERENCES

[1] Du, H., Fan, Z., Yang, L. & Bao, X. (2018). Synthesis and Antimicrobial Activities of Novel 1, 2, 4-Triazole-acyl-hydrazone Derivatives Containing the Quinazolin-4-one Moiety. Chinese Journal of Organic Chemistry, 8(2), 531-538. https://doi.org/10.6023/cjoc201708051

[2] Yilmaz, F. & Menteşe, E. (2017). Synthesis and characterisation of some coumarin-1,2,4-triazol-3-thioether hybrid molecules. Journal of Chemical Research, 41(1), 4-6. https://doi.org/10.3184/174751917X14815427219040

[3] Madeira, C.L., Speet, S.A., Nieto, C.A., Abrell, L., Chorover, J., Sierra-Alvarez, R., & Field, J.A. (2017). Sequential anaerobic-aerobic biodegradation of emerging insensitivemunitions compound 3-nitro-1,2,4-triazol-5-one (NTO). Chemosphere, 167, 478–484. https://doi.org/10.1016/j.chemosphere.2016

[4] Krzmarzick M.J., Khatiwada, R., Olivares, C.I., Abrell, L., Sierra-Alvarez, R., Chorover, J. & Field, J.A. (2015). Biotransformation and degradation of the insensitivemunitions compound 3-nitro-1,2,4-triazol-5-one, by soil bacterial communities, Environmental Science & Technology, 49, 5681–5688. https://doi.org/10.1021/acs.est.5b00511

[5] Özil, M., Balaydın, H.T. & Şentürk M. (2019). Synthesis of 5-methyl-2,4-dihydro-3H-1,2,4-triazole-3-one's aryl Schiff base derivatives and investigation of carbonic anhydrase and cholinesterase (AChE, BuChE) inhibitory properties. Bioorganic Chemistry, 86, 705–713. https://doi.org/10.1016/j.bioorg.2019.02.045

[6] Akin, S., Ayaloğlu, H., Gültekin, E., Çolak, A., Bekircan O. & Yildirim Akatin M. (2019). Synthesis of 1,2,4-triazole-5-on derivatives and determination of carbonic anhydrase II isoenzyme inhibition effects. Bioorganic Chemistry, 83, 170-179.

[7] Paul, A., Anbu, S., Sharma, G., Kuznetsov, M.L., Koch, B., Fatima, M., Da Silva, C.G., Pombeiro A.J.L. (2015). Synthesis, DNA binding, cellular DNA lesion and cytotoxicity of a series of new benzimidazole-based Schiff base copper(II) complexes. Dalton Transactions, 44, 19983–19996.

[8] Qin, Q.P., Meng, T., Tan, M.X., Liu, Y.C., Luo, X.J., Zou, B.Q., Liang H. (2018). Synthesis, crystal structure and biological evaluation of a new dasatinib copper(II) complex as telomerase inhibitor. European Journal of Medicinal Chemistry, 143, 1597–1603. https://doi.org/10.1016/j.ejmech.2017.10.058

[9] Rudrapal, M. & Biplab De, B. (2013). Chemistry and Biological Importance of Heterocyclic Schiff's Bases. International Research Journal of Pure & Applied Chemistry, 3(3), 232-249.

[10] Shiu, K.B., Liu, S.A., & Lee, G.H., (2010). One-pot conditional self-assembly of multicopper metallacycles. Inorganic Chemistry, 49(21), 9902–9908.

[11] Madeira, C.L., Field, A. J., Simonich T.M., Tanguay, R. L., Chorover, J. & Sierra-Alvarez, R. (2018). Ecotoxicity of the insensitive munitions compound 3-nitro-1,2,4-triazol-5-one (NTO) and its reduced metabolite 3-amino-1,2,4-triazol-5-one (ATO). Journal of Hazardous Materials, 343, 340-346. https://doi.org/10.1016/j.jhazmat.2017.09.052

[12] Anouar, E.H. (2014). A quantum chemical and statistical study of phenolic schiff bases with antioxidant activity against DPPH free radical. Antioxidants, 3, 309-322.

[13] Amić, Z. Marković, J.M. Dimitrić Marković, V. Stepanić, B. Lučić, D. (2014). Towards an improved prediction of the free radical scavenging potency of flavonoids: the significance of double PCET mechanisms. Food Chemistry, 152, 578-585.

[14] Lin Lim, F.C.P., Hua, L.M., Tiekink, E.R.T. & Dolzhenko, A.V. (2018). One-pot, microwave-assisted synthesis of polymethylene-bridged bis (1H-1,2,4-triazol-5(3)-amines) and their tautomerism. Tetrahedron Letters, 59, 3792–3796. https://doi.org/10.1016/j.tetlet.2018.09.018

[15] Mohameda, N.G., Shehaa, M. M., Hassana, H.Y.,. Abdel-Hafezb, L.J.M. & Omarc, F.A. (2018). Synthesis, antimicrobial activity and molecular modeling study of 3-(5-amino-(2H)-1,2,4-triazol-3-yl]-naphthyridinones as potential DNA-gyrase inhibitors. Bioorganic Chemistry, 81, 599–611. https://doi.org/10.1016/j.bioorg.2018.08.031

[16] Hu, T.P., Li, M.M., Ya-Ru Huang, Y.R., Gao, L.L., Wang, X.Q., Gao, J.F. & Niu X.Y., (2018). Fluorescent and magnetic properties of three complexes basedon 4,4'-(1H-1,2,4-triazol-1-yl)methylene-bis(benzonic acid). Polyhedron, 151, 306–312. https://doi.org/10.1016/j.poly.2018.05.019

[17] Somagond, S.M., Kamble, R.R., Shaikh, S.K.J., Kumar, S.M., Dasappa, J.P., Byrappa, K., Bayannavar, P.K., Chougala L.S. & Kadadevarmath, J.S. (2018). (E)-N'-(4-nitrobenzylidene)-2-(1-(4-methoxyphenyl)-5-oxo-1H -1,2,4-triazol-4(5H)-yl)acetohydrazide: Synthesis, crystal structure, DFT and Hirshfeld surface analysis. Chemical Data Collections, 13–14, 126–138. https://doi.org/10.1016/j.cdc.2018.02.001

[18] Çetin, A., Korkmaz, A. & Kaya, E. (2018). Synthesis, characterization and optical studies of conjugated Schiff base polymer containing thieno[3,2-b]thiophene and 1,2,4-triazole groups. Optical Materials, 76, 75-80. https://doi.org/10.1016/j.optmat.2017.12.022

[19] Süleymanoğlu, N., Ünver, Y., Ustabaş, R., Direkel, S. & Alpaslan G. (2017). Antileishmanial activity study and theoretical calculations for 4-amino-1,2,4-triazole derivatives. Journal of Molecular Structure, 1144, 80-86. https://doi.org/10.1016/j.molstruc.2017.05.017

[20] Kattimani, P.P., Kamble, R.R., Atukuri, D., Hunnur, R.K., Kamble, A .A. & Devarajegowda, H.C., (2017). C5-Alkyl-1,3,4-oxadiazol-2-ones undergo Dealkylation upon Nitrogen Insertion to form 2H-1,2,4-Triazol-3-ones: synthesis of 1,2,4-triazol-3-one hybrids with riazolothiadiazoles and triazolothiadiazines. Journal of Heterocyclic Chemistry, 54, 2258–2265. https://doi.org/10.1002/jhet.2813

[21] Gökçe, H., Öztürk, N., Ceylan, Ü., Alpaslan, Y.B. & Alpaslan G. (2016). Thiol–thione tautomeric analysis, spectroscopic (FT-IR, Laser Raman, NMR and UV–vis) properties and DFT computations of 5-(3-pyridyl)-4H-1,2,4-triazole-3-thiol molecule. Spectrochimica Acta Part A: Molecular and Biomolecular Spectroscopy, 163, 170–180. https://doi.org/10.1016/j.saa.2016.03.041

[22] Solima, S.M., Hagar, M., Ibid, F. & El Ashry, E.H. (2015). Experimental and theoretical spectroscopic studies, HOMO–LUMO, NBO analyses and thione–thioltautomerism of a new hybrid of 1,3,4-oxadiazole-thione with quinazolin-4-one. Spectrochimica Acta Part A: Molecular and Biomolecular Spectroscopy, 145, 270–279. https://doi.org/10.1016/j.saa.2015.01.061

[23] Arslan, N.B. & Özdemir, N. (2015). Direct and solvent-assisted keto-enol tautomerism and hydrogen-bonding interactions in 4-(m-chlorobenzylamino)-3-phenyl-4,5-dihydro-1H-1,2,4-triazol-5-one: a quantum-chemical study. Journal of Molecular Modeling, 2015 21(1), 19. https://doi.org/10.1007/s00894-015-2574-8

[24] Mohamed, T.A., Soliman, U.A., Shaaban, I.A., Zoghaib, W.M. & Wilson, L.D. (2015). Raman, infrared and NMR spectral analysis, normal coordinate analysis and theoretical calculations of 5-(methylthio)-1,3,4-thiadiazole-2(3H)- thione and its thiol tautomer, Spectrochimica Acta Part A: Molecular and Biomolecular Spectroscopy. 150 339–349.

[25] Boursas, F., Berrah, F., Kanagathara, N., Anbalagan, G. & Bouacida, S. (2019). XRD, FT-IR, FT-Raman spectra and ab initio HF vibrational analysis of bis (5-amino-3-carboxy-1H-1,2,4-triazol-4-ium) selenate dihydrate. Journal of Molecular Structure, 1180, 532-541. https://doi.org/10.1016/j.molstruc.2018.12.037

[26] Medetalibeyoğlu, H., (2015). Bazı yeni 4-[3-(3-metoksibenzoksi)-benzilidenamino]-4,5dihidro-1H-1,2,4-triazol-5-on türevlerinin sentezi, deneysel ve teorik özelliklerinin incelenmesi. Doktora Tezi, Kafkas Üniversitesi, Fen Bilimleri Enstitüsü, Kimya Anabilim Dalı, Kars.

[27] Frisch, M.J., Trucks, G.W., Schlegel, H.B., Scuseria, G.E., Robb, M.A., Cheeseman, J.R., Scalmani, G., Barone, V., Mennucci, B., Petersson, G.A., Nakatsuji, H., Caricato, M., Li, X., Hratchian, H.P., Izmaylov, A.F., Bloino, J., Zheng, G., Sonnenberg, J.L., Hada, M., Ehara, M., Toyota, K., Fukuda, R., Hasegawa, J., Ishida, M., Nakajima, T., Honda, Y., Kitao, O., Nakai, H., Vreven, T., Montgomery, J.A., Peralta, J.E., Ogliaro, F., Bearpark, M., Heyd, J.J., Brothers, E., Kudin, K.N., Staroverov, V.N., Kobayashi, R., Normand, J., Raghavachari, K., Rendell, A., Burant, J.C., Iyengar, S.S., Tomasi, J., Cossi, M., Rega, N., Millam, J.M., Klene, M., Knox, J.E., Cross, J.B., Bakken, V., Adamo, C., Jaramillo, J., Gomperts, R., Stratmann, R.E., Yazyev, O., Austin, A.J., Cammi, R., Pomelli, C., Ochterski, J.W., Martin, R.L., Morokuma, K., Zakrzewski, V.G., Voth, G.A., Salvador, P., Dannenberg, J.J., Dapprich, S., Daniels, A.D., Foresman Farkas, J.B., Ortiz, J.V., Cioslowski, J. & Fox, D.J. (2010).Gaussian 09, Revision B.01, Gaussian, Inc., Wallingford CT,

[28] Keith, T. & Millam, J. (2009). GaussView, Version 5, R Dennington, Semichem Inc, Shawnee Mission, KS.

[29] Wolinski, K., Hinton, J.F. & Pulay, P. (1990). Efficient implementation of the gauge-independent atomic orbital method for NMR chemical shift calculations. Journal of the American Chemical Society, 112, 8251-8260.

[30] Jamróz M.H. (2004). Vibrational Energy Distribution Analysis: VEDA 4 program. Warsaw.

[31] VlčekJr, A. & Záliš, S. (2007). Modeling of charge-transfer transitions and excited states in d6 transition metal complexes by DFT techniques. Coordination Chemistry Reviews, 251 258–287. https://doi.org/10.1016/j.ccr.2006.05.02

[32] Ocak, N., Çoruh, U., Kahveci, B., Şaşmaz, S., Ağar, E., Vázquez-López, E.M. & Erdönmez, A. (2003). 1-Acetyl-3-(p-chlorobenzyl)-4-(p-chlorobenzylidenamino)-4,5-dihydro-1H-1,2,4-triazol-5-one. Acta Crystallographica Section E, 59(6), 750-752.

[33] Çoruh, U., Kahveci, B., Şaşmaz, S. & Kim, Y. (2003). 1-Acetyl-4-(p-chlorobenzylideneamino)-3-methyl-4,5-dihydro-1H-1,2,4-triazol-5-one. Acta Crystallographica Section E, 59(4), 530-532

[34] Mulliken, R.S. (1955). Electronic Population Analysis on LCAO–MO Molecular Wave Functions. The Journal of Chemical Physics, 23 1833–1840. https://doi.org/10.1063/1.1740588

[35] Silverstein, R.M. Webster, F.X. (1998). Spectroscopic Identification of Organic Compound, sixth ed., John Willey & Sons, New York.

[36] Pihlaja, K., Kleinpeter (Eds.), E. (1994). Carbon-13 Chemical Shifts in Structural and Sterochemical Analysis, VCH Publishers, Deerfield Beach.

[37] Fukui, K. (1982). Role of frontier orbitals in chemical reactions. Science 218, 747-754.

[38] Pearson R.G. (1986). Absolute electronegativity, hardness correlated with molecular orbital theory, Proceedings of the National Academy of Sciences of the United State of America, 83, 8440-8441.

[39] Öztürk, N. Alpaslan, Y.B. Alpaslan, G., Alaşalvar, C. & Gökçe, H. (2018). Structural, Spectroscopic (FT-IR, Raman and NMR), Non-linear Optical (NLO), HOMO-LUMO and Theoretical (DFT/CAM-B3LYP) Analyses of N-Benzyloxycarbonyloxy-5-Norbornene-2,3-Dicarboximide Molecule. Süleyman Demirel Üniversitesi Fen Bilimleri Enstitüsü Dergisi, 22(1), 107-120. http://dx.doi.org/10.19113/sdufbed.01322